AGSO

GEOMAT – Modelling of Continental Shelf Sediment Mobility in Support of Australia's Regional Marine Planning Process

P.T. Harris, R. Smith, O. Anderson,
R. Coleman and D. Greenslade

AGSO Record 2000/41

~ G E O S C I E N C E   A U S T R A L I A ~

AUSTRALIAN GEOLOGICAL SURVEY ORGANISATION

AGSO
AUSTRALIAN GEOLOGICAL SURVEY ORGANISATION

AGSO Record Number 2000/41

GEOMAT - Modelling of Continental Shelf Sediment Mobility in Support of Australia's Regional Marine Planning Process

P. T. Harris[1], R. Smith[1], O. Anderson[2], R. Coleman[3,4] and D. Greenslade[5]

1. Antarctic CRC and Australian Geological Survey Organisation, GPO Box 252-80, Hobart, Tasmania 7001, Australia
2. Kort & Matrikelstyrelsen, Geodetic Division, Rentemestervej 8, DK-2400 Copenhagen NV, Denmark
3. Department of Surveying & Spatial Information Science, University of Tasmania, GPO Box 252-76, Hobart, Tasmania 7001, Australia
4. CSIRO, Division of Marine Research, GPO Box 1538, Hobart, Tasmania 7001 Australia
5. Bureau of Meteorology Research Centre, GPO Box 1289K, Melbourne VIC 3001 Australia

AGSO
AUSTRALIAN GEOLOGICAL SURVEY ORGANISATION

Australian Geological Survey Organisation

Chief Executive Officer: Neil Williams

Department of Industry, Science & Resources

Minister for Industry, Science & Resources: Senator The Hon. Nick Minchin
Parliamentary Secretary: The Hon. Warren Entsch, MP

ISSN: 1039-0073
ISBN: 0 642 39860 7

Executive Summary

GEOMAT is a geological-oceanographic computer modelling project which aims to enhance our understanding of the processes controlling sediment mobilisation on the Australian continental shelf. This report describes tidal and surface ocean swell-wave models and their application to studies of shelf sediment mobilisation. The work has been carried out over the past 2 years by a team of collaborators from AGSO, the University of Tasmania, the Australian Bureau of Meteorology and Kort & Matrikelstyrelsen, Geodetic Division in Denmark.

Our models predict that swell wave energy is sufficient to mobilise fine sand (0.1 mm diameter), on at least one occasion during the year March 1997 to February 1998, over 63.5% of the Australian continental shelf. The largest and most powerful waves were able to mobilise fine sand up to a water depth of 148 m in the Great Australian Bight. Tidal currents are capable of mobilising fine sand at least once per semi-lunar cycle (ie. ~2 weeks) over about 56.4% of the shelf.

Overlaying the wave and tide threshold exceedence maps demonstrates that there are areas on the shelf where one process dominates, some areas where tides and waves are of relatively equal importance and still other areas where neither process is significant. We defined 6 shelf regions of relative wave and tidal energy: zero (no-mobility); waves-only, wave-dominated, mixed, tide-dominated and tides-only. The relative distribution of these regions varies with grain size. Inclusion of estimated mean grain size is being undertaken at the present time and this will enhance the usefulness of the regionalisations.

GEOMAT provides a predictive, process-based understanding of the shelf sedimentary system. It helps to explain the distribution patterns of surficial sediments and will probably be useful for mapping biological habitats and communities, although further work is needed to better define these relationships. GEOMAT provides a useful tool that will assist with marine environmental management in general, and with the National Ocean's Office regional marine planning process in particular. It has demonstrated applications to marine engineering projects where shelf sediment mobilisation is of concern and to regional studies of pollution dispersal and accumulation.

Table of Contents

1. INTRODUCTION

Demand is growing for increased and assured access to the ocean and its resources from numerous commercial groups, including fisheries and aquaculture, the petroleum industry, shipping and tourism. Assessing the requirements of these industries in relation to community demands for a clean and healthy ocean environment around Australia is the task of the newly formed National Oceans Office in Hobart. In April, 2000, the National Oceans Office hosted an "Ocean's Forum" which began the process of formulating a series of regional environmental plans, starting with the "Southeast Regional Marine Plan". AGSO has the role of providing the marine geological information that the government requires to facilitate the regional marine planning process and the management of Australia's marine environment.

1.1 A Geological Perspective on Marine Environmental Management

In the broadest sense, "environmental management" is best viewed as "a *process* that begins with *goal setting* and extends through the functions of *information systems, research, planning, development, regulation and financing*" (MacNeil, 1971; p. 5). A major new initiative in Australian marine environmental management is being undertaken currently through a process known as Regional Marine Planning. Regional Marine Plans (RMPs) are vehicles for implementing Australia's Oceans Policy and giving effect to its core vision: *Healthy oceans: cared for, understood and used wisely for the benefit of all now and in the future.*

Within the RMP process, emphasis is placed on the protection and preservation of ecosystems, within the context of the interests of stakeholders (ie. the fishing, shipping and petroleum industries, defence requirements, recreational users, cultural and environmental interests, etc.). The overall approach aims to understand and protect biodiversity, and to integrate economic, environmental, social and cultural objectives governing Australia's ocean domain. The National Oceans Office http://www.oceans.gov.au, an executive agency of the Commonwealth Government, has a coordinating role between governments and stakeholders in the development of each regional marine plan. The first RMP will be developed for the southeast region of Australia.

In practice, the development of RMP's incorporates an assessment of the environmental, economic, social and cultural values, current uses and impacts that are particular to any given region. The size and diversity of Australia's marine environment demands that different management issues and strategies will need to be considered for each region. By definition, ecosystems include living organisms, environments (habitats), and bio-geochemical cycles (Nitrogen, Carbon, Phosphorus, etc) and hence the geosciences make a fundamental contribution to the understanding of these key ecosystem components. Marine geoscience has much to offer in the RMP process in terms of understanding ecosystems and ecosystem response to perturbations (for example, via geochemical cycles and palaeoenvironmental studies).

To protect and preserve biodiversity, governments employ several management measures such as imposition of catch limits, species protection, and most importantly, the declaration of Marine Protected Areas (MPA's). Of particular significance to the present study, however, is the contribution that geoscience can make to the understanding and mapping of marine benthic habitats (ie. facies). It is therefore important that the applications of facies models to environmental management are fully appreciated.

Sound environmental management practices must be based upon a broad foundation of knowledge, a "pyramid-shaped" structure (eg. de Pablo et al., 1994), having a descriptive-observational "information system" at the base and above which are linkages to specific environmental processes that can be modelled. Before the "planning" stage of the management process is reached (and well before the "development" stage) basic descriptive data must be collected and research must be conducted to understand the environmental processes and linkages to the earth's environmental systems (NASA, 1988). It is perhaps one of the major stumbling blocks of marine environmental management in Australia that so much of the essential basic data is yet to be collected; things as elementary as water depth, seafloor sediment type and dominant biota are quite simply not known for large parts of the Australian EEZ.

From a marine geologist's perspective, the fundamental descriptive variables that are needed, at the "information system" level, are the bed morphology, grain properties, sediment composition and biogenic constituents (Fig. 1). This basic, information system, level is best provided through modern geographic information systems (GIS). Components of the Information system may be linked to specific physical, chemical and biological processes, which in various combinations are characteristic of different sedimentary environments. Facies and stratigraphic models are placed at the top of the pyramid (Fig. 1) because they are based upon a synthesis (or "distillation"; Walker and James, 1992) of the descriptive data and of the processes that are specific to a given sedimentary environment.

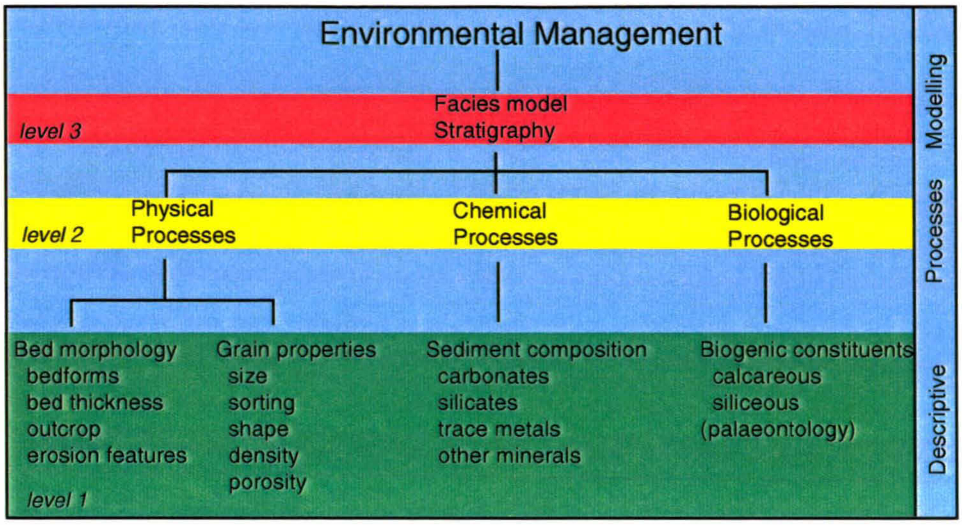

Figure 1. Levels of knowledge related to the work required for different sedimentology studies. Studies may be mainly descriptive (level 1), they may examine one or more sedimentary processes (level 2), or they may use this information to derive a facies (spatial) or temporal (stratigraphic) model (level 3). Environmental management requires knowledge derived from all 3 levels.

There are a number of different sources for the primary descriptive data (Fig. 2). These include remotely sensed images such as LANDSAT, that can be processed to yield other information on seabed types (eg. Rennie et al., 1997). Deep ocean bathymetry data has been greatly enhanced in recent years by the collection of modern swath-multibeam data, which is now available for a large part of the southeast region of Australia. For much of the more shallow sections of the continental shelf and coastal environments, however, there is less data available. Acoustic data on seafloor morphology (eg. sidescan sonar, high resolution seismic data, 3.5 kHz data, etc) has been collected in association with AGSO seismic surveys, port surveys, pipeline and cable routes and for other locations of industrial significance. Seabed sediment samples obtained using cores or surface grabs have been collected systematically over some areas, mainly in the coastal and shelf environments and less frequently on the deeper slope and rise. Much of the data for Australia is contained in the AUSEABED database complied by Dr. Chris Jenkins at Sydney University:
(http://www.usyd.edu.au/su/geosciences/geology/centres/osi/cjj.html>http://www.usyd.edu.au/su/geosciences/geology/centres/osi/cjj.html) Many results of previous workers have already been published in the literature and these will need to be reviewed and incorporated into the overall synthesis of information.

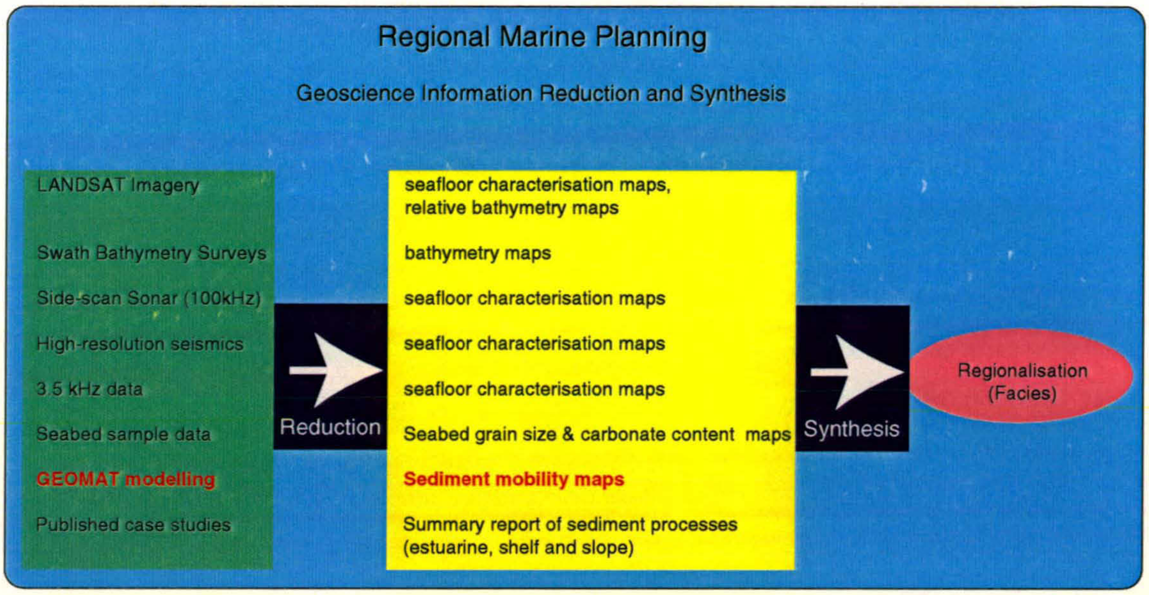

Figure 2. Flow diagram showing the stages of the reduction of specific geoscience data types into maps and spatial information followed by the synthesis of these and other information to produce a regionalisation of sediment facies.

Another kind of information needed for the synthesis of this primary-descriptive type of data is that which relates to sedimentary processes, controlling the introduction, dispersal and deposition of sediments in the marine environment. These processes include the chemical and biological formation and cementation of sediments, biological and physical mixing and transport of grains, etc. A key resource available stems from recent work at AGSO on a project called "GEOMAT". This comprises a GIS-based set of computer programs which simulates the initiation of grain movement on the continental shelf under the influence of tidal current and surface swell wave conditions.

1.2 What is GEOMAT?

GEOMAT (an acronym for "Geological and Oceanographic Models for Australia's Ocean Territory") is an integrated marine geological and oceanographic computer model for marine environmental management. It uses wave and tidal current input data to estimate sediment mobility and the frequency of mobility over continental shelves. Work on GEOMAT began at the Antarctic CRC in 1997 and initially focussed on wave processes using output of global climate models which included estimates of surface swell waves. The first results were published by Harris and Coleman (1998; see Appendix A).

has been suggested that about 80% of the worlds shelves are storm-dominated, 17% are tide-dominated and 3% are ocean-current dominated (Walker, 1984).

During 1999-2000, work on GEOMAT has focussed on the Australian region. The data sets used have been expanded to include the influence of tidal currents and a high resolution wave data set has been included. In this report, we provide a detailed description of GEOMAT, its modelling components, products and applications to the regional marine planning process. In addition, and perhaps most importantly, GEOMAT has the potential to address unresolved questions raised by sedimentologists over the past several decades.

1.3 The science behind GEOMAT

One unanswered question in continental shelf sediment research is "What percentage of the earth's continental shelves are subject to currents strong enough to mobilise the bed sediments (Swift and Thorne, 1991)?" Although it has been suggested that about 80% of the world's shelves are dominated by storm-wave activity, 17% by tidal currents and 3% by ocean-current interactions (Walker, 1984), there has never been a quantitative analysis of continental shelves to determine the spatial distribution of dominant sediment transport processes. The main limitation has been the practical difficulties involved in collecting enough data over the shelf regions to carry out any analyses. In a first attempt at quantifying the influence of the global wave climate on sediment mobility, Harris and Coleman (1998) used wave data generated by a global climate model. These workers found that the wave climatology was such that 0.1 mm diameter quartz sand had the potential to be mobilised on at least one occasion during a 3 year period over 41.6% of the earth's continental shelves.

An assessment of the influence of storms (including tropical cyclones), swell waves, tidal currents and intruding ocean currents on Australian shelf sediment dynamics was proposed by Harris (1995). According to this scheme (Fig. 3), the Australian shelf may be subdivided into areas where storm processes dominate in the mobilisation of sediments (82% of the shelf), where tidal currents dominate (17.4%), and where intruding ocean currents dominate (<1%).

1.3.1 *Storm-Dominated Deposits of the Australian Shelf*

Currents produced during storm events dominate in the erosion and transport of sediment over an estimated 82% of the Australian shelf surface area; storms occur in the form of tropical cyclones and temperate storms. The energy expended and the amount of sediment transported during one storm event may equal many months (or years) of non-storm background processes. Even on highly dynamic tidally influenced shelves, the effect of a storm is to initiate sediment movement at even greater water depths and at greater rates in shallower depths than is experienced under normal conditions. Storm dominated shelves may experience less than one or as many as four or five storm events per year which cause sediment transporting flows.

Sediments on the southern parts of Australia's shelf are arranged in zones which trend parallel to the coast, reflecting the dominance of currents related to ocean swell and storms (Fig. 3). Examples of studies which have documented the development of shelf storm deposits include those of the Rottnest Shelf (Collins, 1988), the Lacepede Shelf (James *et al.*, 1992) and the New South Wales Shelf (Davies, 1979; Black and Oldman, 1999). In these locations, long-period swell waves cause nearly continuous reworking of sediments on the inner shelf, winnowing away fine grained sediments and leaving a sorted sandy sediment in the current affected depth zone. Muddy sediments are deposited below this depth; they are accumulating on the middle New South Wales shelf in 60-130m depth, and on the higher energy Lacepede shelf they are deposited in deeper water, below 140m. In general, the facies are aligned spatially such that they trend parallel to the coast and regional isobaths (eg. Fig. 4).

Tropical cyclones are the cause of storm events in much of northern Australia (Fig. 3). They are associated with atmospheric low pressure systems and attain mean wind speeds of at least 63 km/hr. The sections of the shelf most frequently affected by cyclones are the North West Shelf with up to 25 cyclones/decade, and the Great Barrier Reef with up to 15 cyclones/decade (Lourensz, 1981). These shelf areas are not affected greatly by swell generated in a major ocean basin. This pattern is represented in significant wave height data obtained from satellites; whereas significant wave heights are less than 1.5m for 50-70% of the time in northern Australia, they are larger than 3.5m for 30-50% of the time along much of the southern Australia shelf (McMillan, 1982; Fig. 3).

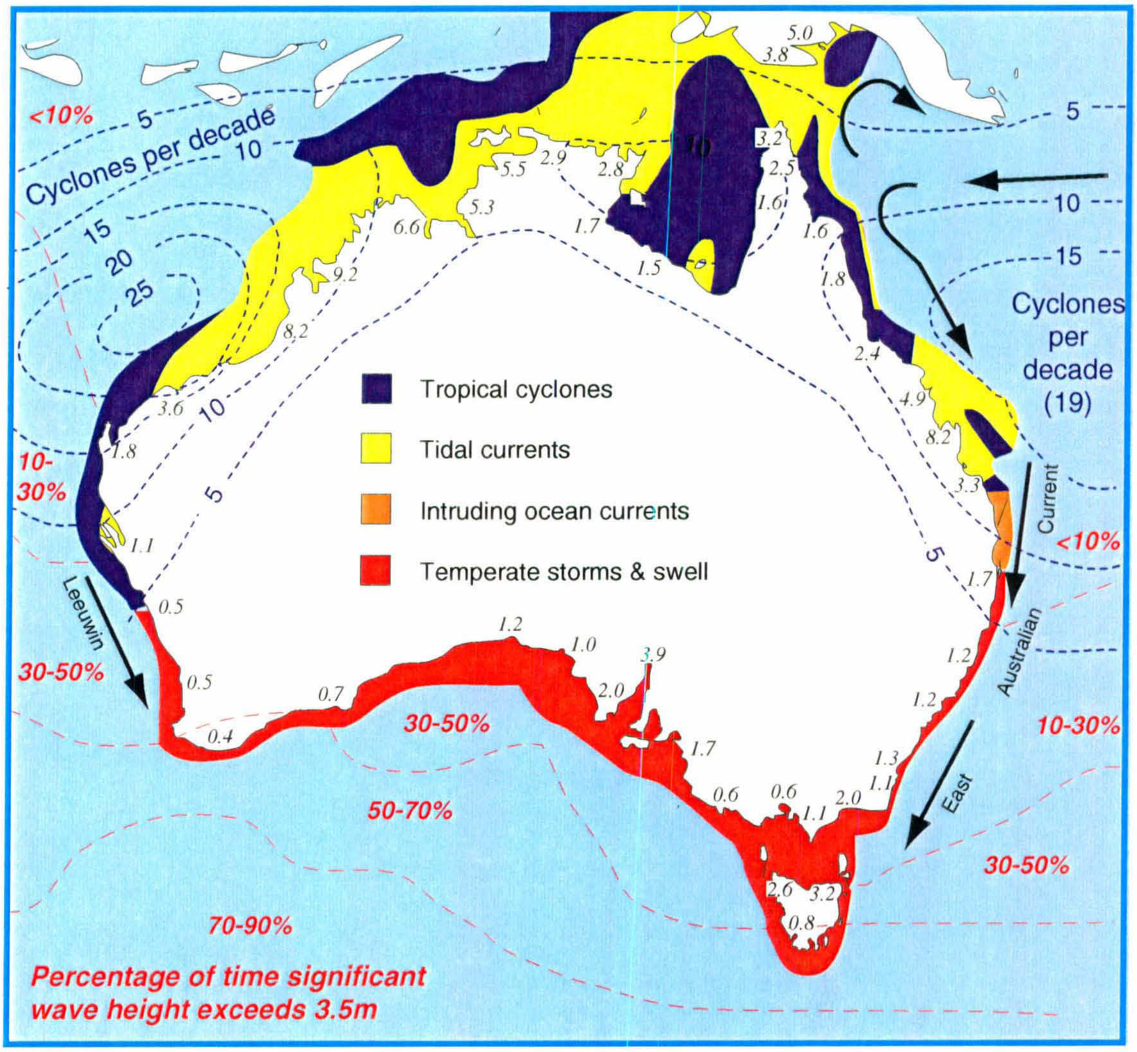

Figure 3. Division of the Australian shelf into regions in which sediment transport is caused mainly by tidal currents (17.4% of the shelf area), currents derived from tropical cyclones (53.8%), ocean swell and storm generated currents (28.2%) and intruding ocean currents (0.6%), after Harris (1995). Contours of tropical cyclone frequency per decade are from Lourensz (1981) and contours for significant wave height percentage exceedence are from McMillan (1982). Mean spring tidal ranges indicated along the coastline are derived from the Australian National Tide Tables. The location and direction of flow of major ocean currents are indicated.

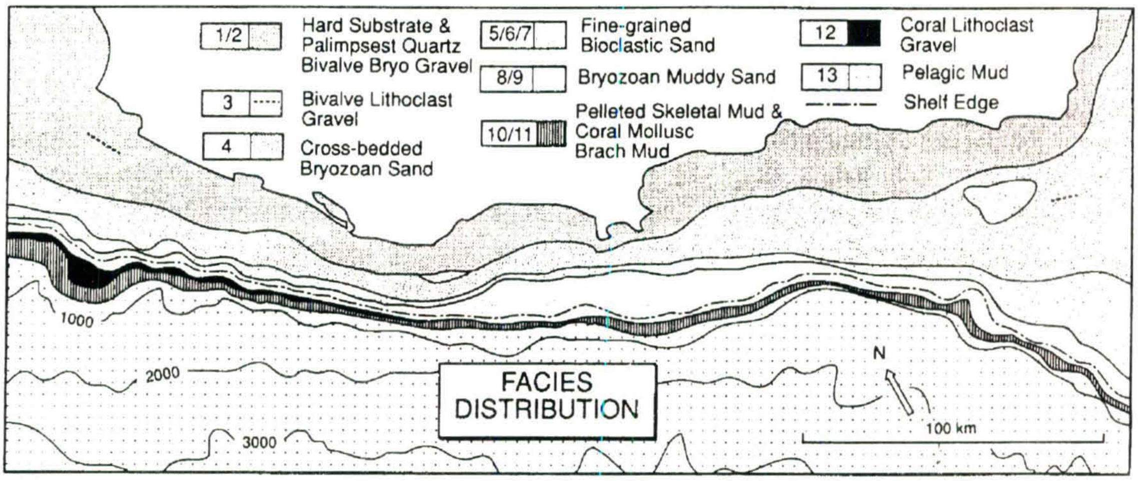

Figure 4. Surficial sediment facies on the Otway continental shelf (after Boreen et al., 1993). Note facies are aligned parallel to the coast.

Tropical cyclones induce strong currents which erode and transport sediment over a wide area. Current measurements, obtained in the Gulf of Carpentaria during one tropical cyclone, recorded near bottom currents with hourly averaged speeds up to 6 times larger than background current speeds (Church and Forbes, 1983). In the Great Barrier Reef, one cyclone is reported to have caused the erosion on the mid-shelf of a sediment layer averaging 6.9cm in thickness and to have transported sediment a minimum distance of 15km (Gagan *et al.*, 1990). Modelling studies by Hearn and Holloway (1990) on the North West Shelf have shown that, under the influence of tropical cyclones, strong westward flowing coastal and inner shelf currents are established between the eye of the cyclone and the coast. Such cyclone-induced currents are clearly a significant factor affecting sediment movement on cyclone-dominated shelves, but they may also influence the long-term (net) sediment movement on some otherwise tidally-dominated sections of the shelf.

1.3.2 *Tidally-Dominated Deposits of the Australian Shelf*

Tidally-dominated shelves occur generally where the mean spring tidal range measured along the coast exceeds 4m (*macrotidal*). Around Australia, tidal ranges >4m occur along the northwestern coastline between Port Hedland and Darwin, reaching a maximum range of around 9.2m in King Sound (Fig. 3). The southern Great Barrier Reef coastline is macrotidal, with a tidal range of 8.2m in Broad Sound. In the Fly River Estuary (Gulf of Papua) tidal ranges are 5m. Tidal currents are also an important sand transporting agent in *mesotidal* (2-4m tidal range) areas such as Torres Strait, Bass Strait and Moreton Bay (Brisbane). Tidal currents are able to dominate sand transport in *microtidal* areas (tidal range <2m) in restricted cases, where coastal geometry affords shelter from ocean generated swell and wind-driven currents. Such is the case in many bays (eg. Shark Bay), the approaches to some major ports (eg. Port Phillip Bay, Melbourne) and in partly enclosed Gulfs (eg. Spencer Gulf, Gulf St. Vincent and the Gulf of Carpentaria). Tidal currents are accelerated as they flow over and between shelf edge barrier reefs; thus sediment transport is affected by tides along the shelf edge over much of the Great Barrier Reef (Fig. 3). In total, sediment transport is dominated by tidal currents on about 17.4% of the Australian shelf.

Tidally dominated shelves exhibit discrete zones of seabed scouring and erosion, associated with an area where tidal currents reach a maximum speed (Fig. 5). An important distinction is that tidal facies have boundaries that are aligned more or less at right angles to the coast (cf. Figures

4 and 5). Seabed sediments are arranged in a divergent pattern reflected by an increasing supply of sand of decreasing grain size with increasing distance away from the scour zone (Johnson *et al.*, 1982). Such diverging bedload transport patterns are known as *bedload partings*. Examples of areas where tidal currents have produced such bedload parting facies are found in the Torres Strait (Fig. 5) and Gulf of Carpentaria regions (Harris, 1994). In these areas, tidal currents are accelerated as they flow through constricted channels located between islands and reefs. The zones of maximum tidal current speed are sometimes related to tidal amphidromic points. These are a type of standing wave node in which sea level change is small but current speeds are large; two such amphidromic points are found in the Gulf of Carpentaria (Harris, 1994).

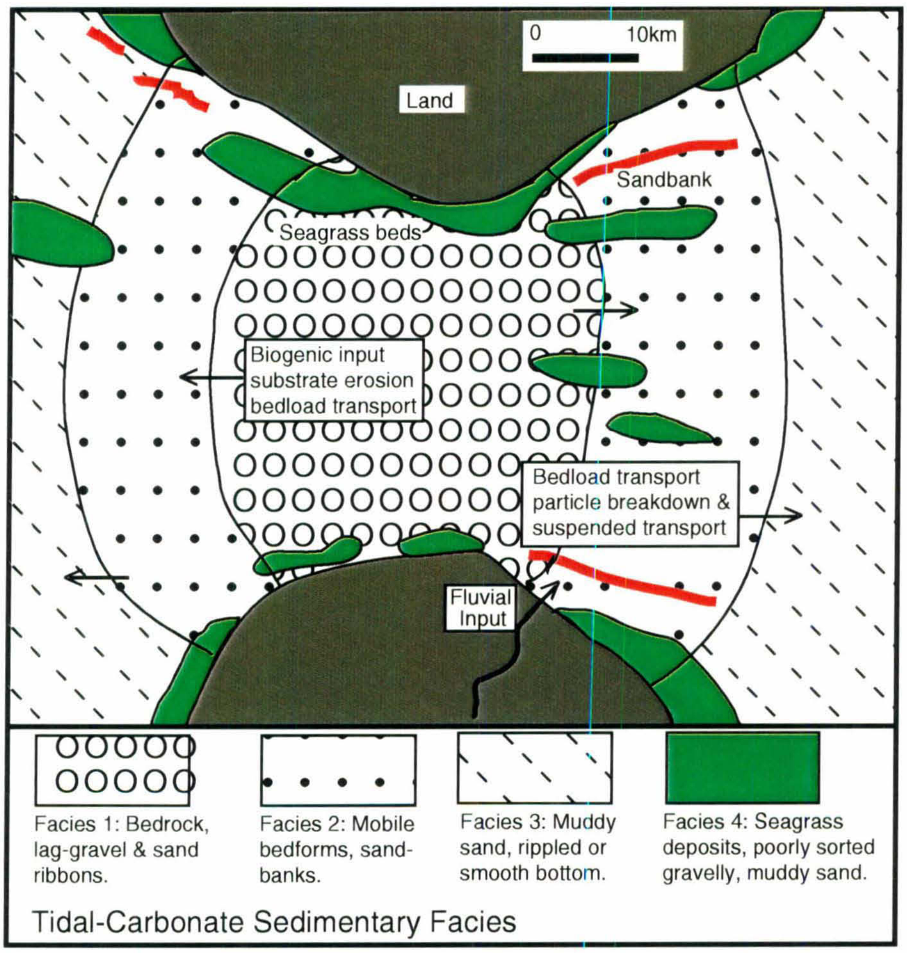

Figure 5 Succession of facies associated with tidal scour zones and bedload partings in a tropical to sub-tropical environment where seagrass beds are also characteristic (after Harris, 1994).

1.3.3 *Shelves Dominated by Intruding Ocean Currents*

Sediment transport and dispersal, controlled by intrusive ocean currents, affects >1% of the Australian shelf (Fig. 3). The only location where such currents are known to dominate sediment movement around Australia is the shelf offshore from Fraser Island, where the southward flowing East Australian Current intrudes onto the shelf (Harris et al., 1996). Sidescan sonar and seabed photographs, obtained during the 1980 cruise of the German research vessel *Sonne* to the northern NSW - southern Queensland region, show the development of large submarine dunes at depths as great as 80m, but more typically in the 40 to 50m range (Jones and Kudras, 1982). Dune morphologies indicate a general southward transport of sand, which Gordon and Hoffman (1986) related to the effect of the East Australia Current. The Leeuwin Current may have a similar effect over parts of the Western Australia shelf, but further research is needed to confirm this.

2. METHODS

2.1 Threshold exceedence due to swell waves

Using Airy, first-order wave theory (Komar and Miller, 1973), we have estimated the wave-induced threshold for specific grain sizes. Currents produced by the passage of a shallow water wave are reduced to backward and forward motions, having an *orbital diameter* d_o. Over the time interval of the wave period T, the velocity at a fixed observation point will vary from zero to some maximum value U_{max} given by:

$$U_{max} = \pi d_o / T = \pi H / [T \sinh (2\pi h / \lambda)] \qquad (1)$$

where H is the wave height, h is the water depth, λ is the wavelength of the surface gravity wave and sinh is the hyperbolic sine function. When the bottom current reaches a certain speed, the bed sediment is mobilised and a threshold value (U_{cr}) is exceeded. Although more accurate estimates of U_{max} are possible by using a spectral wave current model (Madsen, 1994), the necessary wave data are not available; the estimate of U_{max} derived from equation 1 gives an accurate result away from the shoreface zone and under the near-threshold and deep water shelf conditions that are of interest in the present study (Hardisty, 1994).

In this study, surface wind speed estimates generated by the Australian Bureau of Meteorology's regional atmospheric model provided input to the Wave Model, WAM (Hasselman et al., 1988; Komen et al., 1994) to yield estimates of mean wave height and period. The data are 6-hourly predictions of Significant Wave Height (SWH) mean wave period, grided at 0.1° (11 km) spatial resolution, for the period March 1997 to February 1998, inclusive. The WAM model is run operationally at many forecasting centres around the world, including a version at the Australian Bureau of Meteorology. When compared to observations of SWH from wave-rider buoys around the Australian coast, the *rms* error of forecast SWH is approximately 0.5m. The source terms and propagation terms are integrated every 5 minutes. In terms of the wave spectrum, the directional resolution is 15° and there are 25 frequency bins ranging from 0.0418 Hz to 0.4114 Hz. This represents wave periods from approximately 24 seconds to 2.5 seconds. Fields of SWH, mean wave direction and mean period are output every 6 hours.

This high-resolution wave model is nested within a regional wave model, which spans the oceans around Australia, ranging from 60°S to 12°N and from 69°E to 180°. The spatial resolution of the regional model is 1° and the spectral resolution is (necessarily) the same as the spectral resolution of the high-resolution wave model. This larger scale model provides the boundary conditions for input to the high-resolution model. The regional wave model is in turn nested within a 3° resolution global model.

Winds used to force the high-resolution model and the regional model were obtained from hindcasts of the operational regional atmospheric model, LAPS (Puri *et al.* 1998). These wind fields are provided at 3-hourly intervals and are at a spatial resolution of 0.75°. The wind fields are bi-linearly interpolated to the wave model grid. The global wave model is forced with hindcast winds from the global atmospheric model, GASP (Seaman *et al.* 1995). The 10m surface winds are extrapolated from the lowest level of the atmospheric models using Monin-Obukhov theory with empirical stability functions (Garratt, 1992).

Although we are concerned here with the impact of the water waves on the bed sediment, the seafloor in turn has an effect on the surface waves. The major impact on the modelled wave height due to the water depth is that when $h < \lambda/4$ (approximately), an extra source term must be included in the model, representing the dissipation of wave energy due to bottom friction. Other shallow water effects, such as depth-induced breaking are not included in WAM, and for this reason, a water depth of approximately 20m is considered to be the shallowest depth to which it is possible to run WAM successfully.

2.1.1 *Estimation of wave threshold exceedence*

The threshold speed (U_{cr}) is a function of the wave period, boundary layer thickness, bed roughness, grain density and shape, water viscosity and whether or not the grains are cohesive or cemented (eg. Grant and Madsen, 1979, 1986; Hammond and Collins, 1979; see review of Hardisty, 1994). Simplified empirical threshold equations have been published by Clifton and Dingler (1984), for flat-bed, spherical, cohesionless, quartz silt and fine sand (density = 2.65 g/cm^3 and grain size $D < 0.05$ cm in diameter), given as:

$$U_{cr} = 33.3\,(TD)^{0.33} \quad (2)$$

and for coarser sand and gravel where D > 0.05 cm:

$$U_{cr} = 71.4\,(TD^3)^{0.143} \quad (3)$$

Variations in water viscosity (a function of temperature and salinity) are not accounted for in these threshold equations (Clifton and Dingler, 1984). Estimates of most variables required to solve Equation 1 can only be provided from computer models. Satellite altimetry data are useful for estimating the significant wave height ($H_{1/3}$) but cannot provide estimates of wave period or wavelength. Empirical graphs for significant wave height versus wave period show a wide scatter and so even on a local basis, it is not possible to assign a significant period to a given significant wave height.

The other variable needed in equation 1 is the water depth (h). For this we used the AGSO bathymetry data base, which are interpolated to a grid spacing of 0.01° (0.6 nautical miles or ~ 1 km). Next, we extrapolated the wave data 0.1° (11 km) grid to combine it with the 1 km bathymetry grid, and solved equations 1-3 at six-hourly intervals. The number of times that the threshold value was exceeded at each bathymetric grid point was summed to derive threshold exceedence maps of the world's continental shelf region for grain sizes of 0.01 mm, 0.1 mm, 0.5 mm, 1 mm and 2 mm.

2.2 Threshold exceedence due to tidal currents

Threshold exceedence was estimated for unidirectional, steady flow conditions using the empirical curves of Miller et al. (1977). This graph is based on the results of selected open-channel, straight-sided flume experiments conducted by various investigators, using standard laboratory conditions (ie., an initial flat bed, cohesionless quartz spheres under steady, fresh water flows at 20° C). The data specify an empirical formula which gives threshold exceedence for quartz spheres (< 2mm in size) under the above described laboratory conditions, as: $U_{100} = 122.6\,D^{0.29}$ where U_{100} is the threshold current speed referenced to 100 cm above the seabed and D is the grain diameter in mm.

Hourly-averaged, tidal current speeds were estimated using a hydrodynamic tidal model for the Australian shelf, derived specifically to meet the spatial-temporal requirements of the present study. GEOMAT incorporates a program that tallies the occurrences when the depth-averaged current speed predicted by the model exceeds the threshold speed for specified grain sizes. This analysis yields an estimate of the percentage time of threshold exceedence for 5 selected grain sizes of 0.01 mm, 0.1 mm, 0.5 mm, 1 mm and 2 mm.

2.2.1 *Tidal hydrodynamic model*

The linearized shallow water equations are typically assumed for tidal modelling with parametrized corrections for dissipation, tidal loading and ocean self attraction. To a good approximation, the tidal fields $u(\phi,\lambda)$ at a frequency ω satisfy the linearized shallow water equations, for the effects of open ocean self attraction and tidal loading [Hendershott, 1981] subject to boundary condition on M*O*

$$Su = f_o \qquad \begin{vmatrix} u.n = 0 \text{ on } f\,O_{coast} \\ h = h_o \text{ on } f\,O_{open} \end{vmatrix} \qquad (4)$$

where *O* is the full domain represented by the global oceans, f_o is the astronomical forcing and where the indices for position (ϕ,λ) have been omitted for convenience.

The model has two types of boundaries M*O*. The rigid boundaries along coastlines MO_{coast} and the open boundaries along the (northern) edge of the model domain MO_{open}. The coastline boundary condition is no flow normal to the coast, as $n = (n_x, n_y, 0)$ is the direction normal to the rigid boundary. Along the open boundary the conditions are specified through the elevation at each grid cell using an existing ocean tide model (e.g. the model of Schwiderski).

The Laplace tidal operator *S* for linearized shallow water equations is given by

$$S = \begin{vmatrix} i\omega + K & -f & gHG*\nabla_x \\ f & i\omega + K & gHG*\nabla_y \\ \nabla_x\cdot & \nabla_y\cdot & i\omega \end{vmatrix} \qquad (5)$$

where *H* is ocean depth, *f* is the Coriolis acceleration, ω is the constituent frequency, ∇_0 and ∇ represent the two dimensional divergence and gradient operators on the spherical earth, *K* represent dissipation and *G** represents convolution with the Green's function for tidal loading and ocean shelf attraction (Hendershott, 1972).

represent dissipation and G^* represents convolution with the Green's function for tidal loading and ocean shelf attraction (Hendershott, 1972).

The forcing parameter f_o for the astronomical potential given by Cartwright (1993) was used. This parameter includes a correction for earth tide potentials. Convolution with the Green's function for tidal loading and ocean shelf attraction G^* was treated using the simple scalar correction factor $\sigma = 0.9$.

The AGSO bathymetry on a 1 minute (1.8 km) grid was used for the model. However, this database suffers from frequent loss of coverage for several regions in the deep ocean. Consequently it was supplemented with data obtained from the National Geophysical Data Center (NGDC) depth model for depths greater than 2000 meters.

Dissipation is a crucial parameter, and a wide range of formulations have been suggested in the literature. For this model a dissipation model which decreases with the square of the depth has been used:

$$K = K_1 \;/\; (\max(H, H_0))^2 \qquad (6)$$

This parametrization is defined by the drag coefficient K_0 and a minimum depth H_0 above which the dissipation is defined to be constant. The drag coefficient was selected as $K_1 = 0.05$ and the minimum depth of $H_0 = 20$ meters. This parameter choice seemed to work well for most regions .

2.2.2 *Data used in the tidal model*

In the present analysis height observations from tide gauge or satellite have been used (Fig. 6). The height observations from satellite were taken from the ocean altimeter Pathfinder products for TOPEX/POSEIDON exact repeat missions. The Pathfinder data sets are designed to assist the research community providing long time-series data processed with stable calibration and community consensus algorithms. A full description of the data sets, their editing and testing are too lengthy to report here, but can be found through the NASA Pathfinder homepage at http://neptune.gsfc.nasa.gov/ocean.html@

Data were processed using the provided standard corrections. These were: geophysical corrections (solid earth tide, ocean tide, load tide, pole tide, cross track geoid correction and a 100% inverse barometer correction); media corrections (ionosphere, wet and dry troposphere); and instrumental corrections (sea state bias and instrumental corrections). The orbits were based on the JGM-3 earth gravity model. The Pathfinder data are distributed as stacked normal point data interpolated along the ground track for each satellite individually. Observations outside a threshold limit of three times the standard deviation were removed and finally the quasi-stationary sea surface height in each normal point was removed by removing the mean value. All available T/P and ERS-1 data were used, whereas only the first 44 repeats of GEOSAT were used.

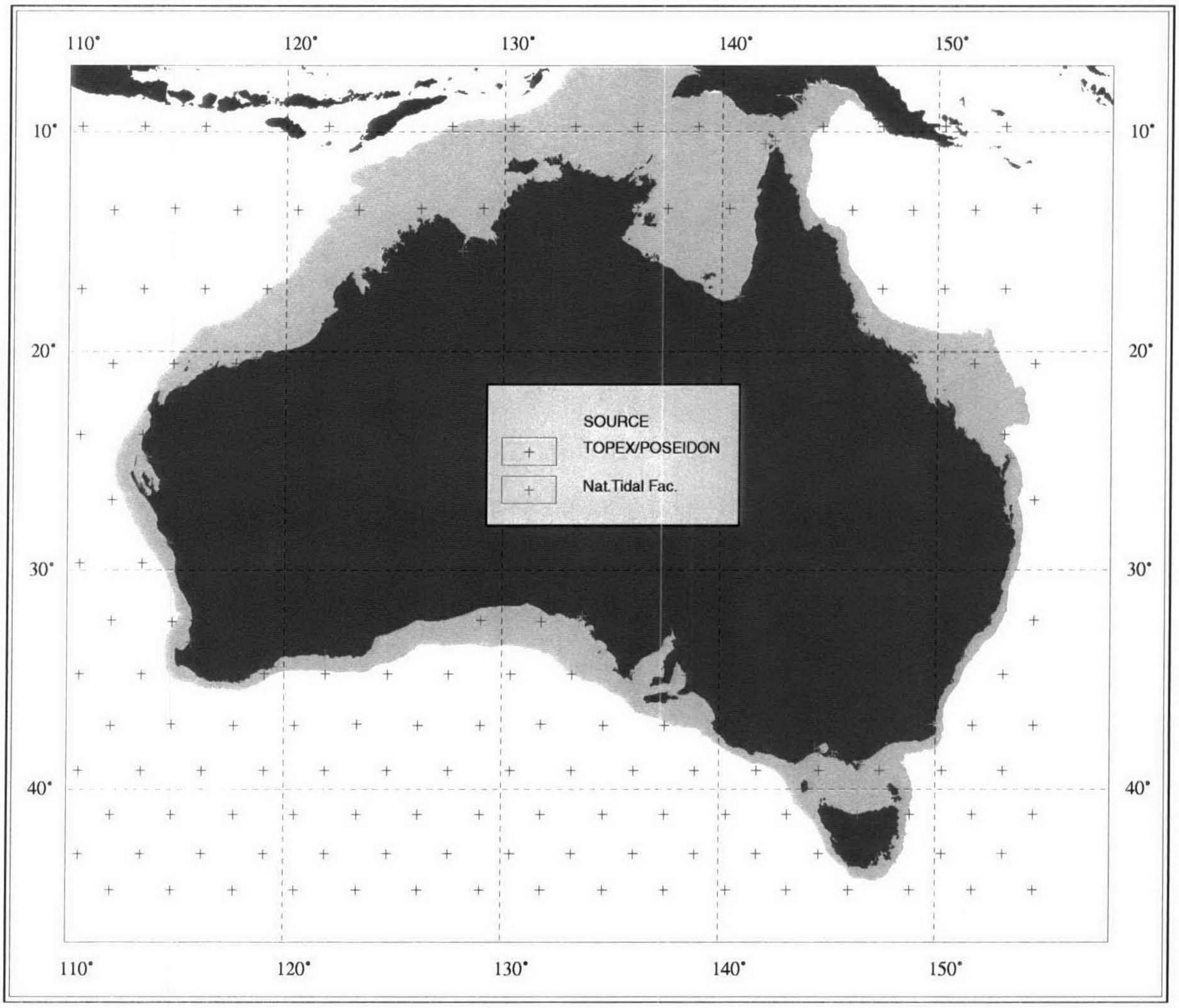

Figure 6. Location of ocean altimeter TOPEX/POSEIDON satellite cross-over points and coastal tide gauge stations used in the present study to force the tidal model.

Finally the crossover locations were computed and the observations were interpolated onto these locations. In each of the crossover locations the harmonic constituents for the major ocean tide constituents were then deduced using the response method (Munk and Cartwright, 1966) with the orthotide extension by Groves and Reynolds (1975). A total of 179 crossover solutions obtained from TOPEX/POSEIDON altimetry was used for the present model.

The National Tidal Facility provided a set of harmonic tidal constituents for the primary ports of Australia. This data set consist of 57 locations. From this data set a further 16 observations of the harmonic constituents were obtained very close to the coast where the coverage of the TOPEX/POSEIDON altimetry was poor. This gave a total of 195 observation of the ocean tide that was nudged into the hydrodynamic model. The location of the combined data set is seen in Figure 6.

2.2.3 *Estimation of tidal current threshold exceedence*

An extended region surrounding Australia was used to include observations from the TOPEX/POSEIDON satellite. The region was limited by the following latitudes: 0S - 45S and longitudes 109E - 160E. The latitude resolution of the model was 1/15 degree corresponding to 7.4 km at the equator and 5.2 km at the southern latitude. The resolution in the longitude direction was constantly 7.4 km (1/15 degree). The resulting model had 750 by 660 cells which meant that a solution could be obtained for one constituent on a Sun Sparc 20 workstation as a overnight job.

The model was set up to include the major 7 constituents M2, S2, N2. K2, K1, O1, Q1. P1 as well as 34 minor constituents could then deduced from admittance interpolation in the final model. The solution was obtained using time stepping on an Arakawa C grid by applying periodic forcing and then explicitly time stepping from homogenous initial conditions. The solution was achieved in 10,000 time steps using a step length of 15 seconds. After a spin-up time of 1,000 time steps the harmonic solutions obtained at crossover and pelagic tide gauge location were nudged into the model.

Using 10,000 time steps corresponds to letting the model run for 170.000 seconds which is equivalent to 2 days which should be adequate for obtaining a reasonable stable accurate solution for each constituent. The time step for this model is somewhat shorter than has been reported by other modellers. However due to the nudging and in order to keep the system stable, a very short time step was needed. The model used in the present analysis had open boundaries all around the edges of the grid. The global ocean tide model version AG95.1 was used to provide boundary elevations (Anderson et al. 1995). At the open boundary the model elevation field is substituted with the elevation field of the open boundary model in each time step.

The computer model was used to derive a spring-neap cycle (roughly two weeks) of hourly-averaged tidal current speeds. The problem of calculating the bottom stress using modelled current speeds is that the effect of the benthic boundary layer is difficult to model in deep water (eg. Pingree and Griffiths, 1979). The tidal model used here generated depth-averaged, hourly-averaged currents, and it ignores the effects of bottom roughness elements and other bathymetric features that can affect the velocity profile.

Based on the threshold curve for unidirectional currents published by Miller et al (1977) occurrences of threshold exceedence were tallied for the hourly current speed at each grid point to then generate a percentage of threshold exceedence map of the Australian continental shelf.

2.3 Relative significance of wave -vs- tidal current threshold exceedence

Shelves may be affected by tides or waves (or both) but the important issue is which process dominates over the other on the Australian continental shelf? In the case of the wave data used here, threshold exceedence by waves occurring during any 6 hour period will register as an "event". The number of events per year yields a percentage of time of wave threshold exceedence for a given grid point.

For tides, threshold exceedence by the hourly-averaged, maximum bottom stress over a spring-neap cycle implies that movement occurs at least every fortnight (or 26 times per year). Thus, the main difference between wave and tide affected shelf areas is that, whereas tidal exceedence is periodic (fortnightly), the wave exceedence is episodic (or seasonal?). The sources of error in the analysis are thus also different for each case.

Our approach will be to assess the relative importance of each category (wave- or tide-dominated) by taking into account the percentage of time that each process is effective in mobilising the seabed sediments. The analysis was carried out for each modelled grid point and the data were used to generate maps showing the spatial distribution of wave- and tide-dominated threshold exceedence.

3. RESULTS

3.1 Waves

3.1.1 *Mean and maximum wave height and period*

The distribution of annual mean wave height and period around Australia (Figs. 7A and B) exhibits a pattern of greater heights and longer periods in the southern waters than in the northern waters[1]. The largest and longest period waves are found off the west coast of Western Australia, in the Southern Bight and off western Tasmania. Relatively low mean heights and shorter periods are found in northern waters, particularly the North West Shelf, Arafura Sea and Gulf of Carpentaria. These results are generally consistent with previous studies of waves on the continental shelf around Australia (eg. Louis and Radok, 1975; McMillan, 1982; Wolanski, 1985). Some interesting features of the data (Figs. 7A and B) include the prediction of quiet zones on the lee sides of islands and within protected embayments. Examples are the relatively low wave energy zones on the eastern side of King and Flinders Islands in Bass Strait. Since diffraction is not accounted for in the wave model used here, these zones are probably overestimated to a certain extent.

The maximum wave height and period maps (Figs. 8A and B) show a similar pattern as the mean distribution, with generally greater heights and longer periods in the southern than in the northern Australian waters. An exception to this is the interesting maximum wave height peak located off the southern Great Barrier Reef, associated approximately with the Marion Plateau (Fig. 8A). The model predicts that 6-hourly averaged swell waves between March 1997 to February 1998 (the time period studied) reached a maximum height of up to 15 m in this region. This height (>15 m) is associated with Hurricane wind conditions, according to the Beaufort Wind Scale, and it would be expected that individual peak wave heights would have been as much as twice this height (~30 m) during such extreme events. The maximum wave period corresponding with this area does not appear to exceed around 12 to 15 seconds (Fig. 8B).

A second region where wave heights are higher than might be expected is in the central Gulf of Carpentaria. Whereas the annual mean wave height in the Gulf is less than 2 m (Fig. 7A), the

[1] In Figure 7 and throughout this report, the offshore limit of the continental shelf is defined as the 500 m isobath for the purposes of our modelling exercise.

maximum heights appear to exceed 8 to 10 m locally (Fig. 8A) although the maximum wave period in this area does not appear to greatly exceed the mean (cf. Figs. 7B and 8B).

3.1.2 *Threshold exceedence due to swell waves*

The distribution of threshold exceedence due to swell waves, calculated for five difference grain size classes over the 12 month-period March 1997 to February 1998 are shown in Figures. 9A-E. Our modelling suggests that fine sand (0.1 mm) was mobilised at least once during this one year period over 63.5% of the Australian continental shelf (Table 1). Note that the estimated areas are for assumed grain sizes and show only the possibility of mobilising a certain grain size if it were present at a given location on the shelf. The results generally demonstrate a landward succession of zones of increasing threshold exceedence, which is particularly clear on broad, shallow shelves (ie.the Great Barrier Reef, Torres Strait and Gulf of Papua).

The location where the most powerful waves in the oceans around Australia are found varies from year to year, depending on the occurrence of storms and prolonged high wind speeds over a large fetch (eg. Vincent, 1986; Harris and Coleman, 1998). The maximum wave height and period occurring on the shelf translates into a maximum water depth of shelf sediment mobilisation (for a given grain size), and this location varied depending on grain size in the data we analysed. Our results indicate that waves were strong enough to mobilise 0.01 mm (silt) to a depth of 185 m in the Southern Bight whereas 0.1 mm (fine sand) was mobilised to a depth of 148 m in the Southern Bight (Table 1).

3.2 Tides

3.2.1 *Maximum tidal current speeds*

Based on the modelling results of the present study, the distribution of maximumtidal current velocity on the Australian shelf has been calculated. Generally, the strongest currents are located on the shelf areas where there is a macrotidal range (ie mean spring tidal range > 4 m; Fig. 10). Along the northwestern coastline of Australia, a maximum spring tidal range of 12.5m is reached in Collier Bay, King Sound (Fig. 10), which is the largest range attained in Australia (Easton, 1970). On the adjacent shelf, our modelling results show maximum tidal current speeds ranging up to around 1.5 m/s (Fig. 11). The coastline in eastern Queensland is also macrotidal, with a tidal range of up to 8.2m in Broad Sound (Cook and Mayo, 1978). In the Fly River Estuary (Gulf of Papua) tidal ranges are amplified to 5m (Wolanski and Eagle, 1991). In these areas, the adjacent shelf is characterised by relatively high maximum tidal currents (Fig. 11).

Table 1. Shelf areas where threshold is exceeded by swell waves for five grain size classes. The maximum depth and coordinates of threshold exceedence for each grain size is also shown.

% exceedence	Area km2	%Shelf	Max Depth	X-coord	Y-coord	Grain Size mm
<=1%	633200	24.88	-185.000	131.825	-33.555	0.01
>1, <=10%	570800	22.43				0.01
>10, <=50%	445300	17.50				0.01
> 50, <100%	195700	7.69				0.01
100	13900	0.55				0.01
<=1%	701000	27.54	-148.100	114.545	-34.055	0.1
>1, <=10%	540700	21.24				0.1
>10, <=50%	294600	11.58				0.1
> 50, <100%	74400	2.92				0.1
100	5300	0.21				0.1
<=1%	680800	26.75	-128.200	141.255	-38.445	0.5
>1, <=10%	484300	19.03				0.5
>10, <=50%	138500	5.44				0.5
> 50, <100%	30200	1.19				0.5
100	1400	0.06				0.5
<=1%	598100	23.50	-114.300	141.275	-38.445	1
>1, <=10%	385700	15.15				1
>10, <=50%	65000	2.55				1
> 50, <100%	13900	0.55				1
100	300	0.01				1
<=1%	486100	19.10	-100.360	141.255	-38.395	2
>1, <=10%	235900	9.27				2
>10, <=50%	33100	1.30				2
> 50, <100%	5900	0.23				2
100	0	0.00				2

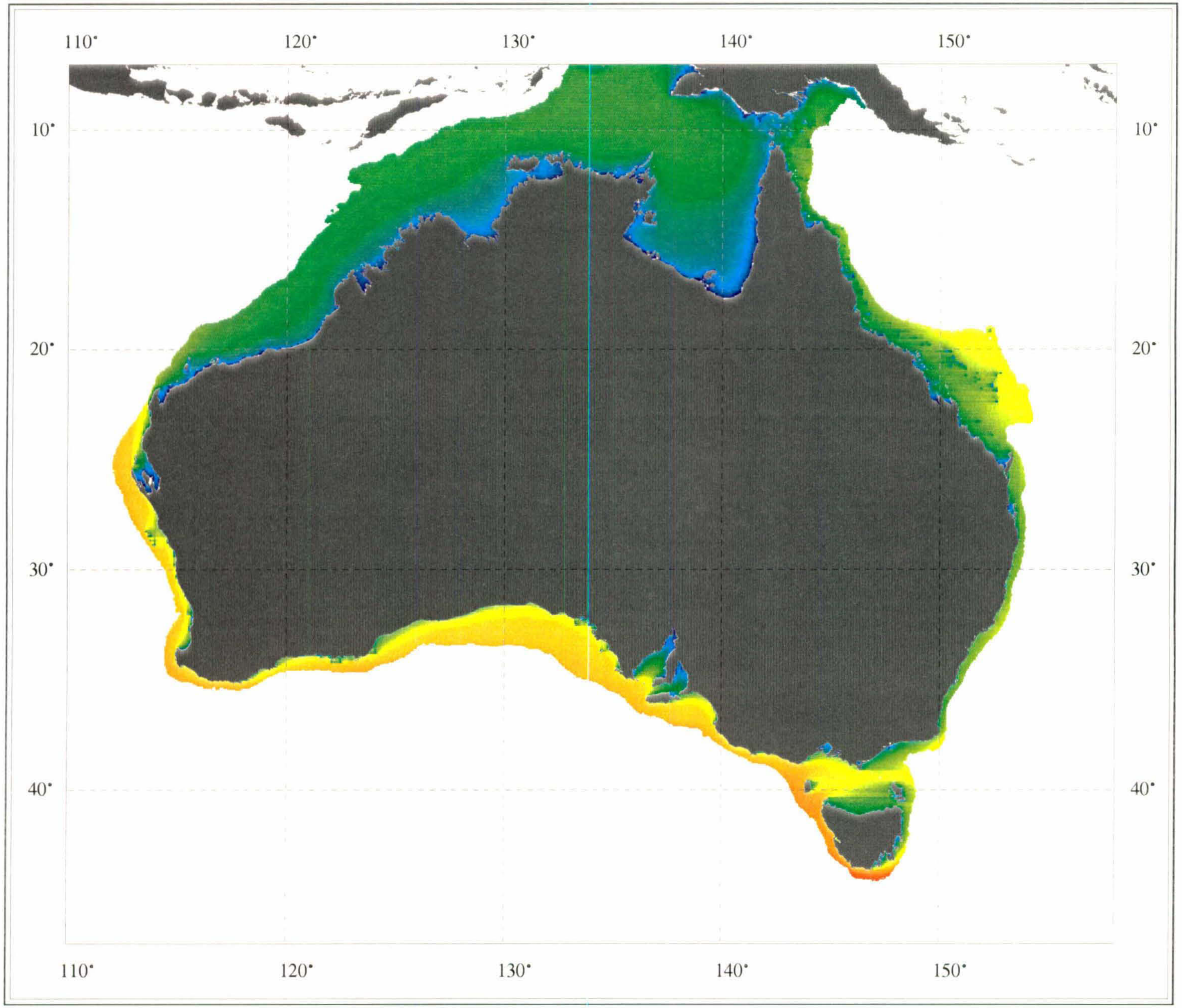

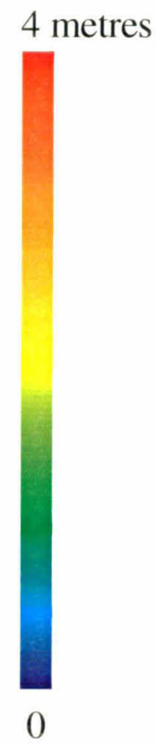

Figure 7A.

Annual Mean Wave Height (m).

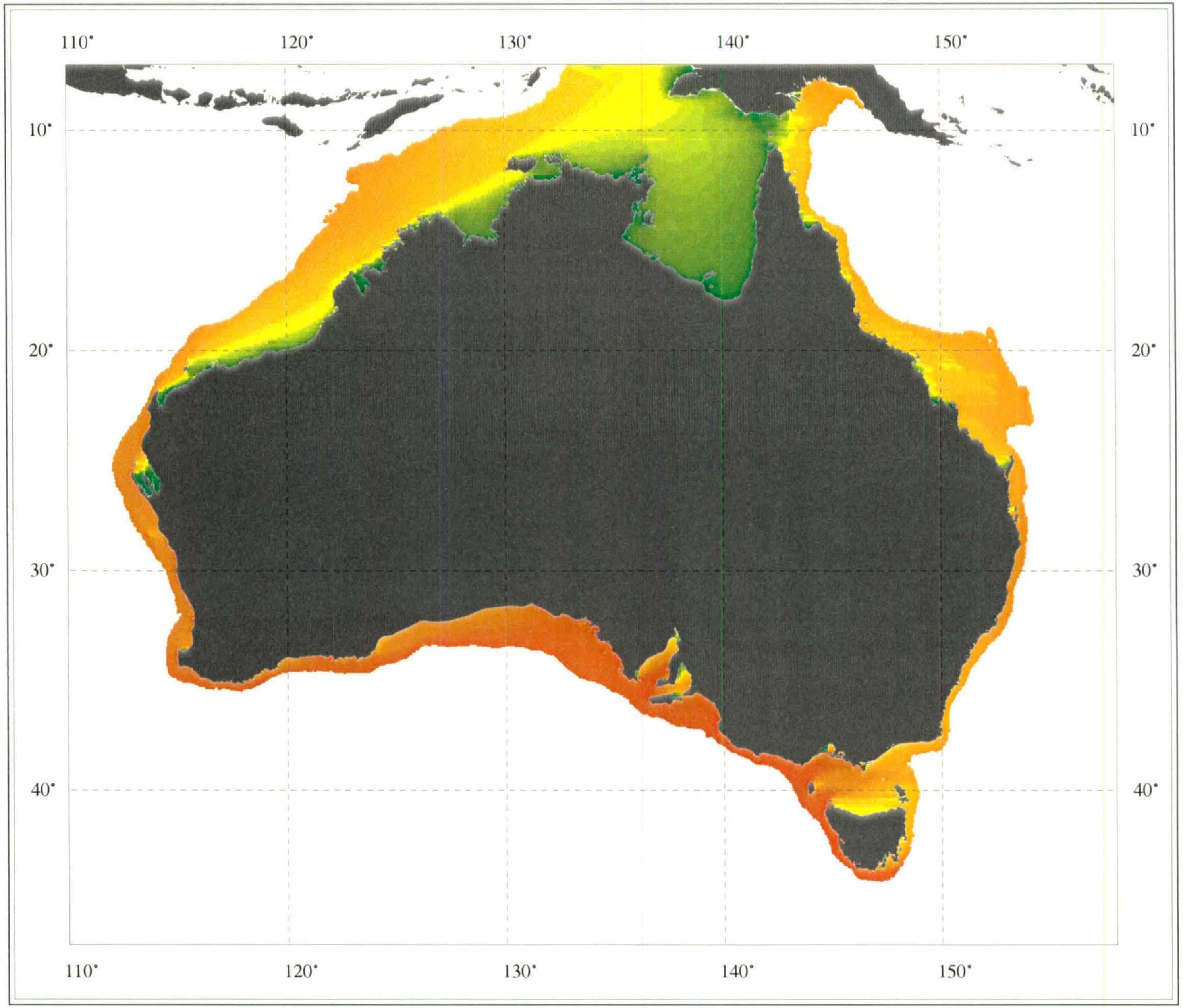

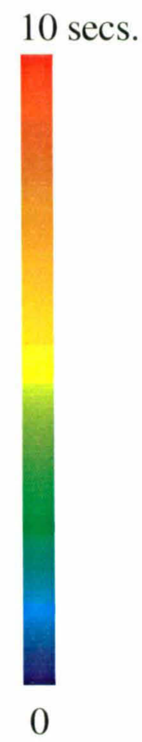

Figure 7B.

Annual Mean
Wave Period (sec).

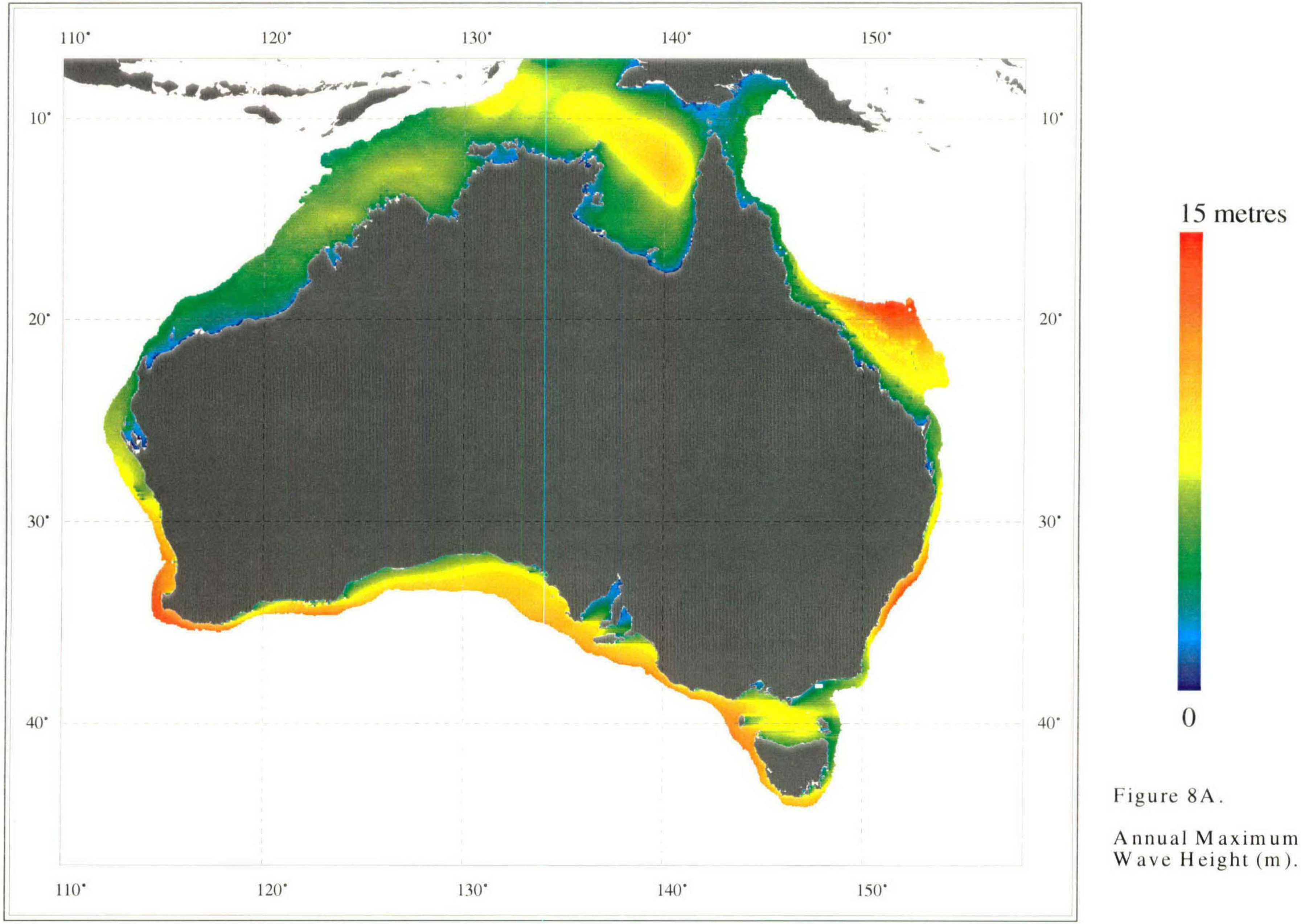

Figure 8A.

Annual Maximum Wave Height (m).

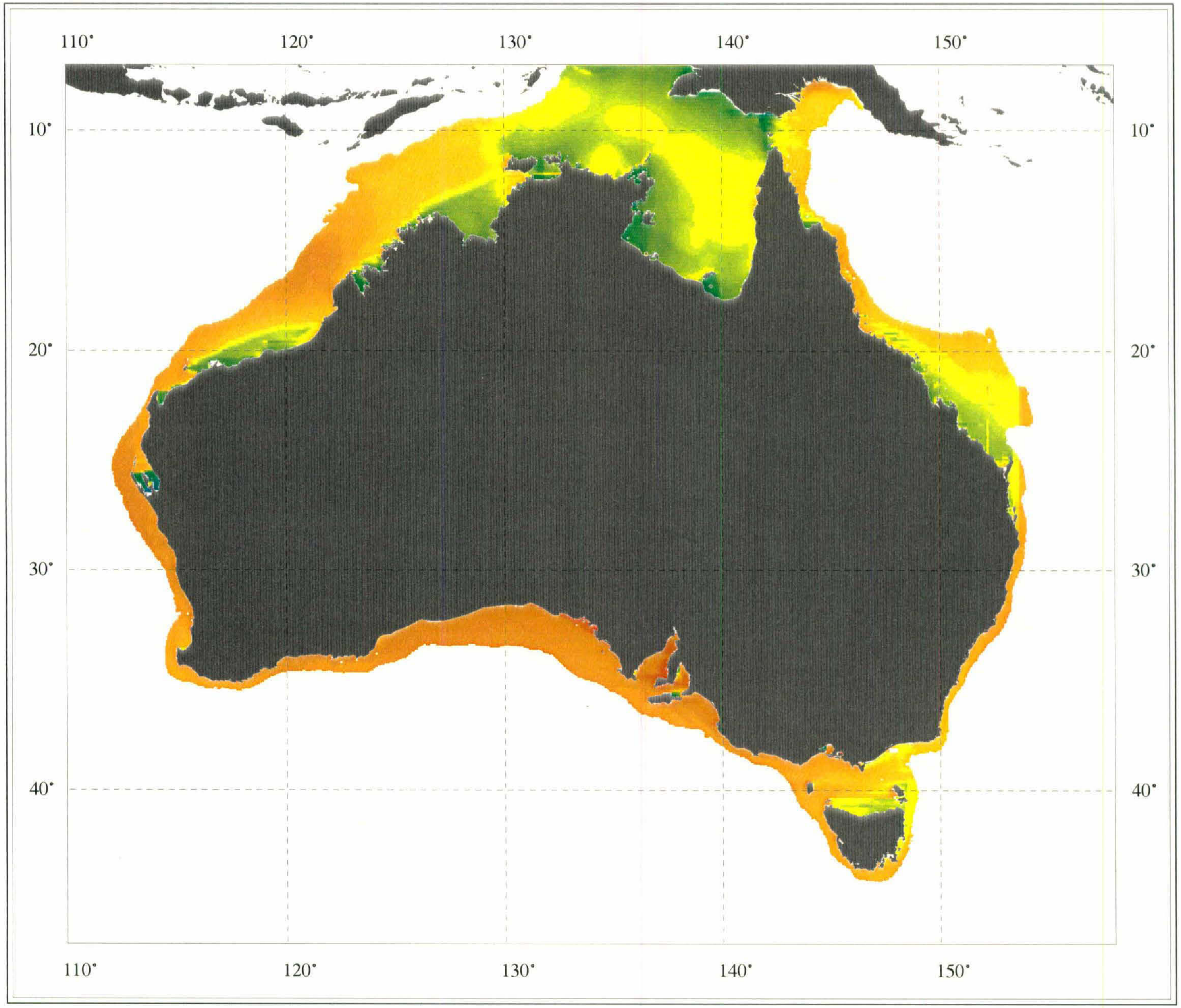

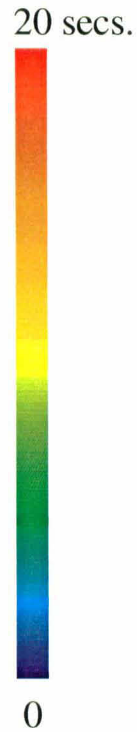

Figure 8B.

Annual Maximum Wave Period (sec).

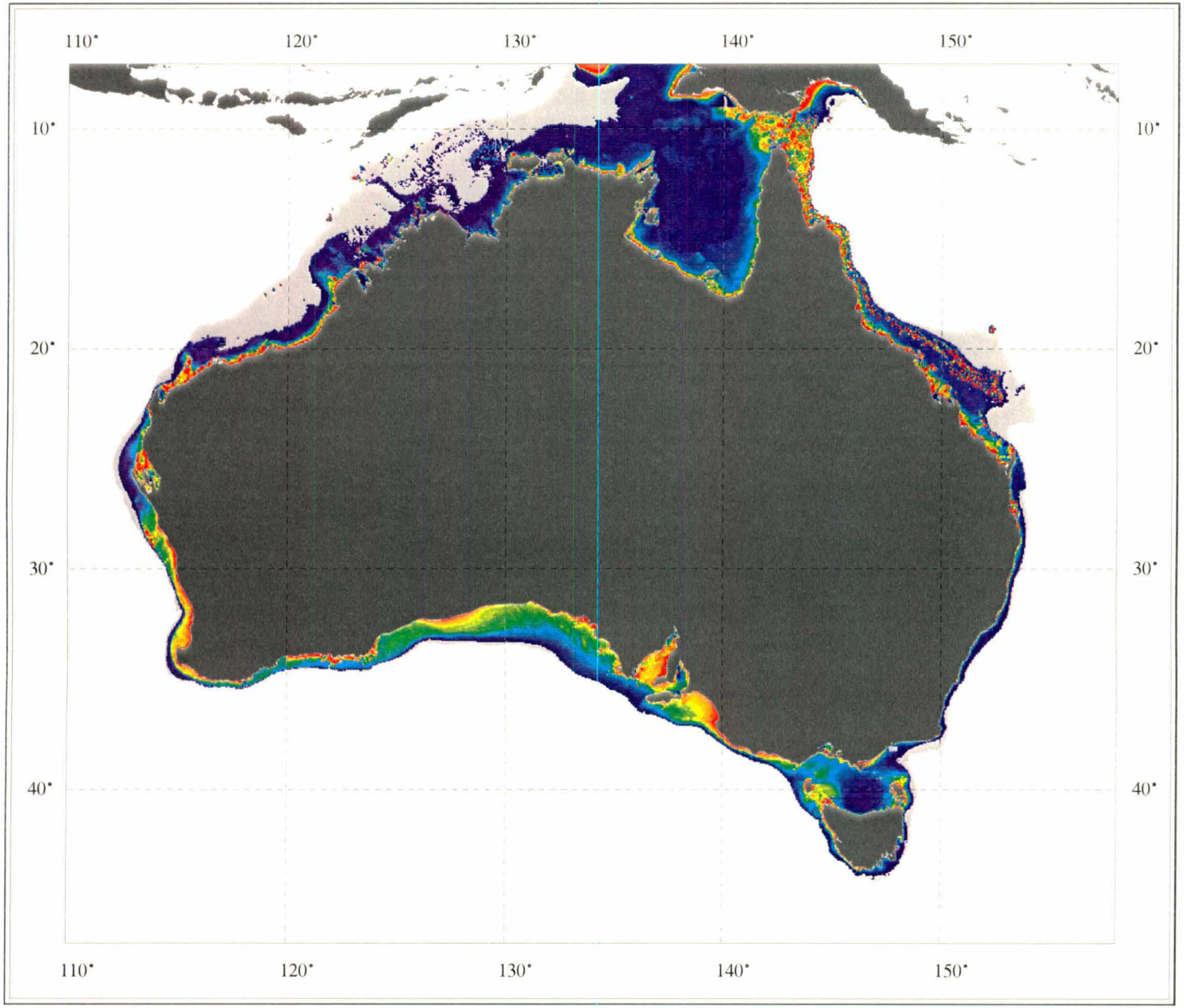

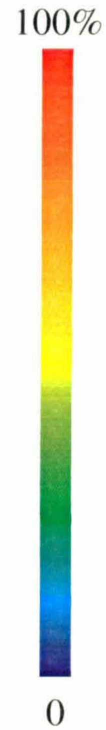

Figure 9A.

Wave Induced Exceedance 0.01 mm grain size.

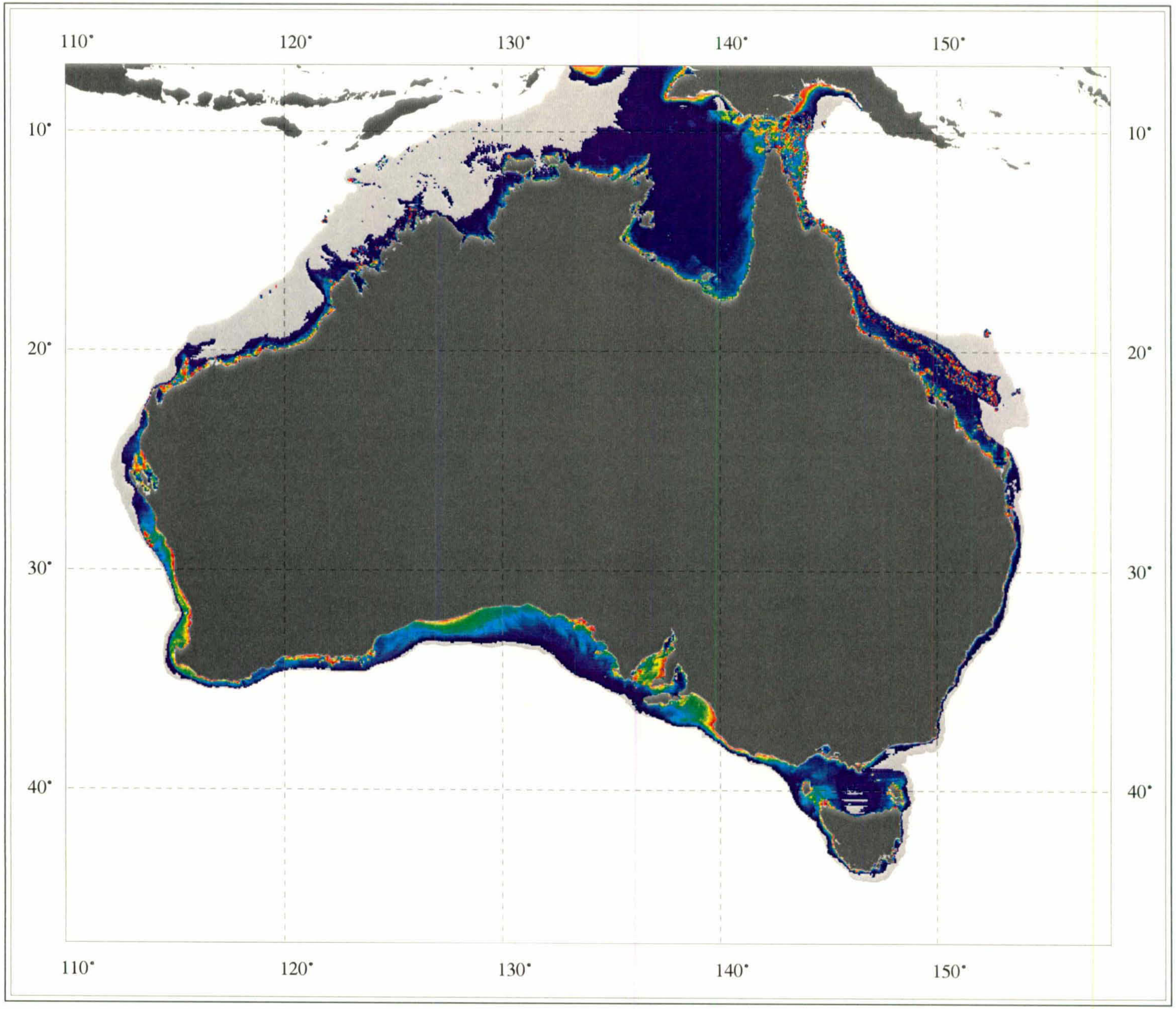

Figure 9B.

Wave Induced
Exceedance
0.1 mm grain size.

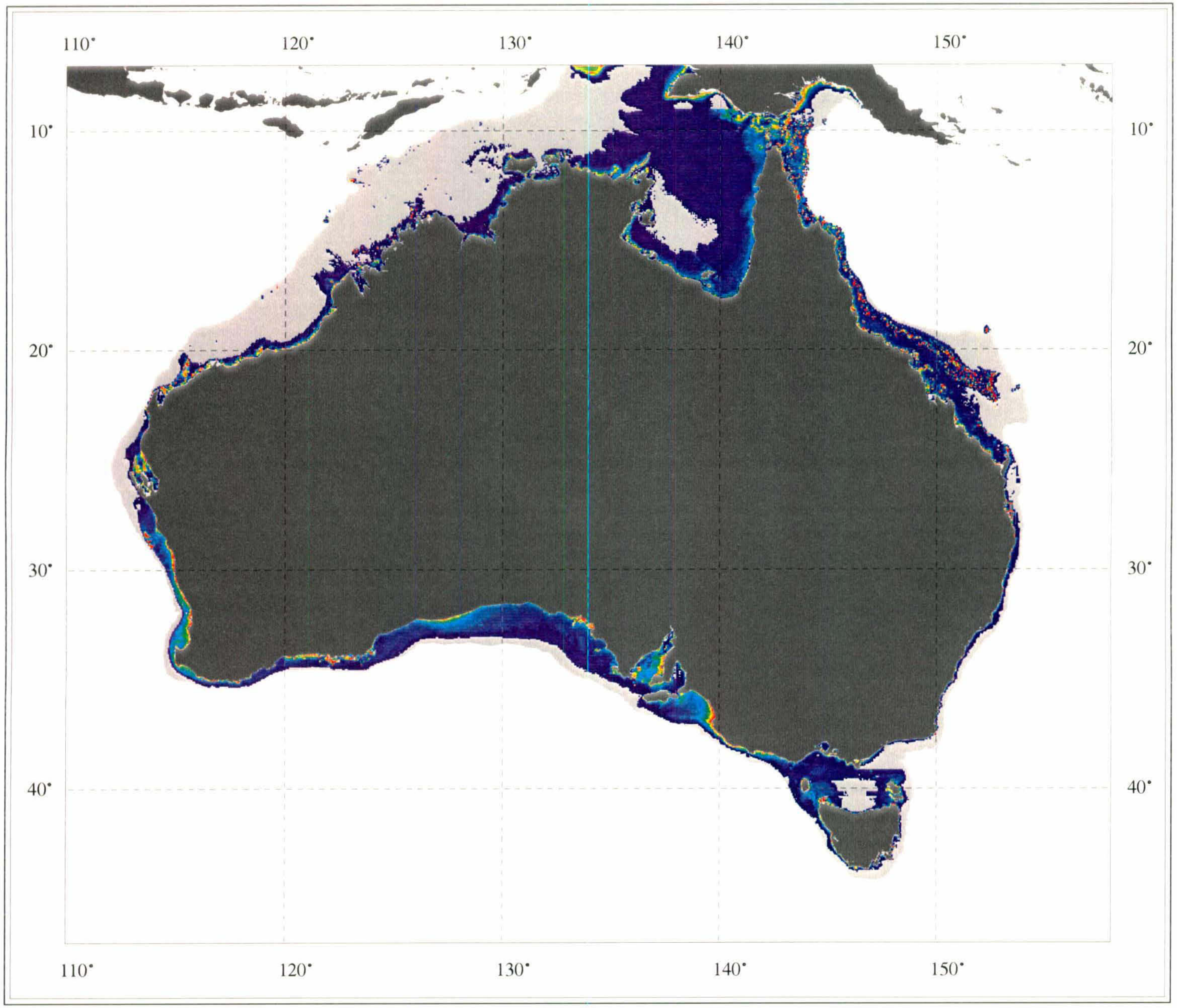

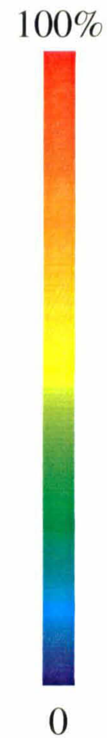

Figure 9C.

Wave Induced Exceedance 0.5 mm grain size.

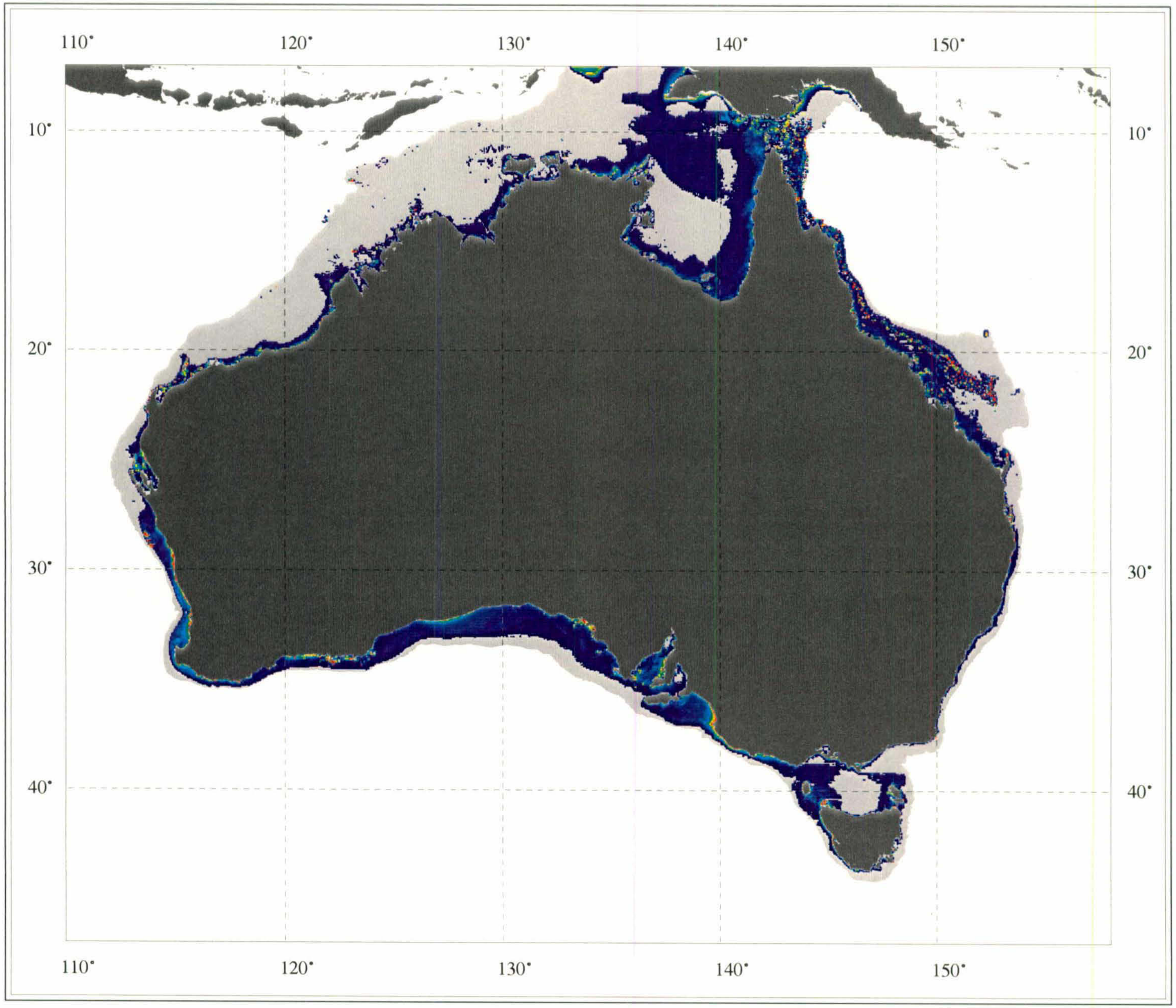

Figure 9D.

Wave Induced Exceedance 1.0 mm grain size.

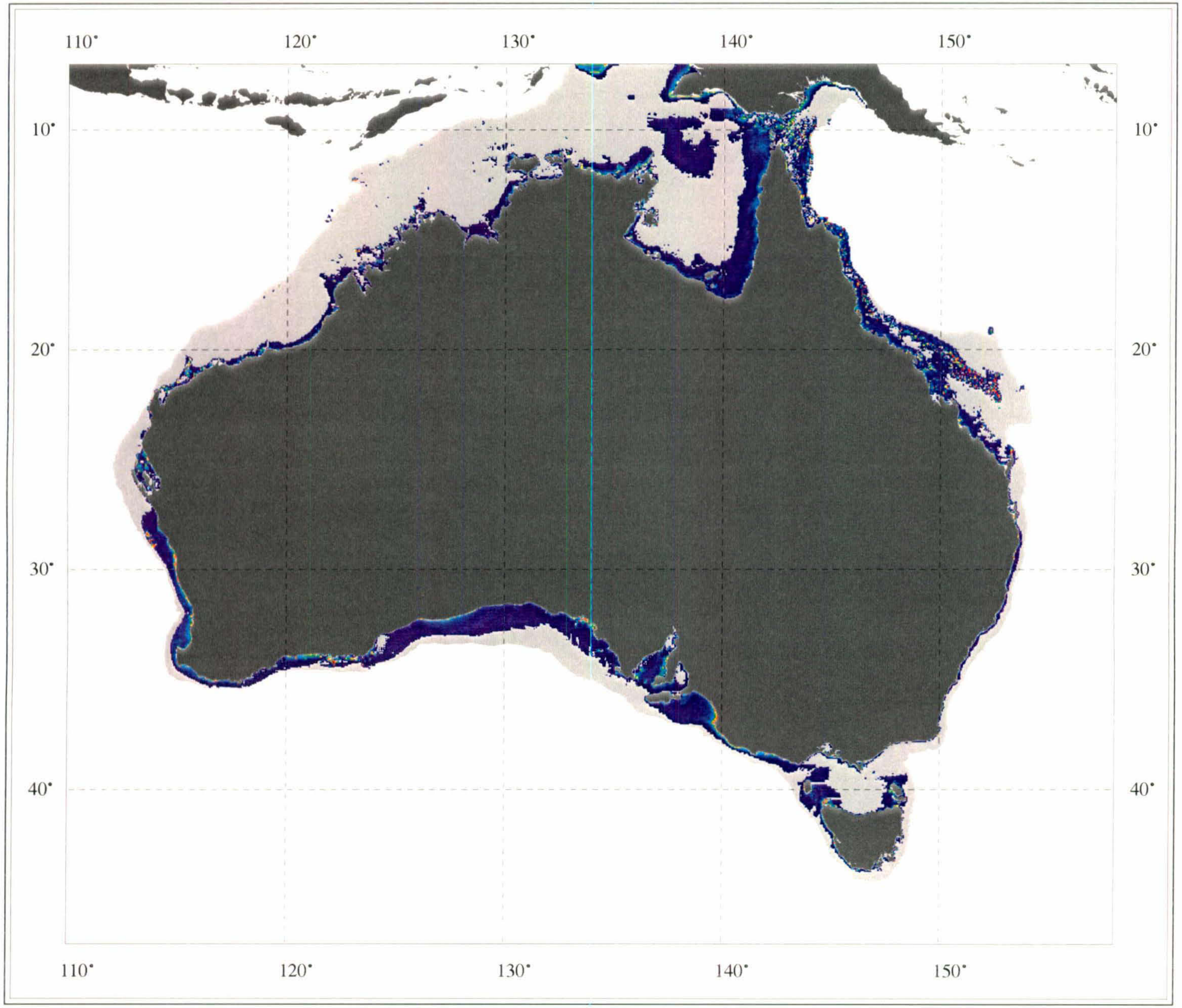

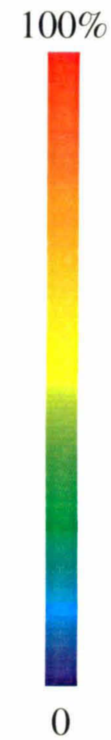

Figure 9E.

Wave Induced Exceedance 2.0 mm grain size.

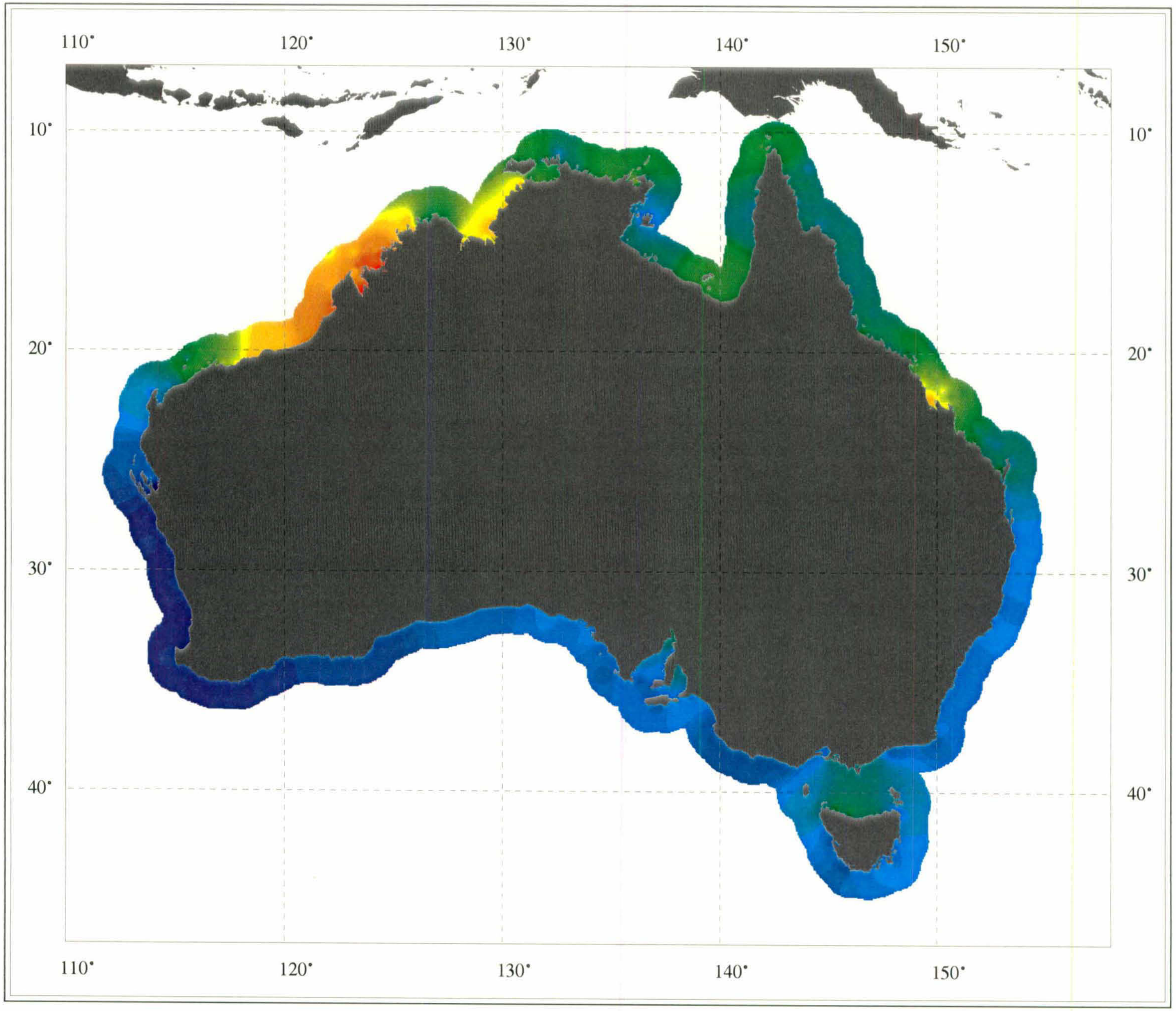

Figure 10.

Tidal Range

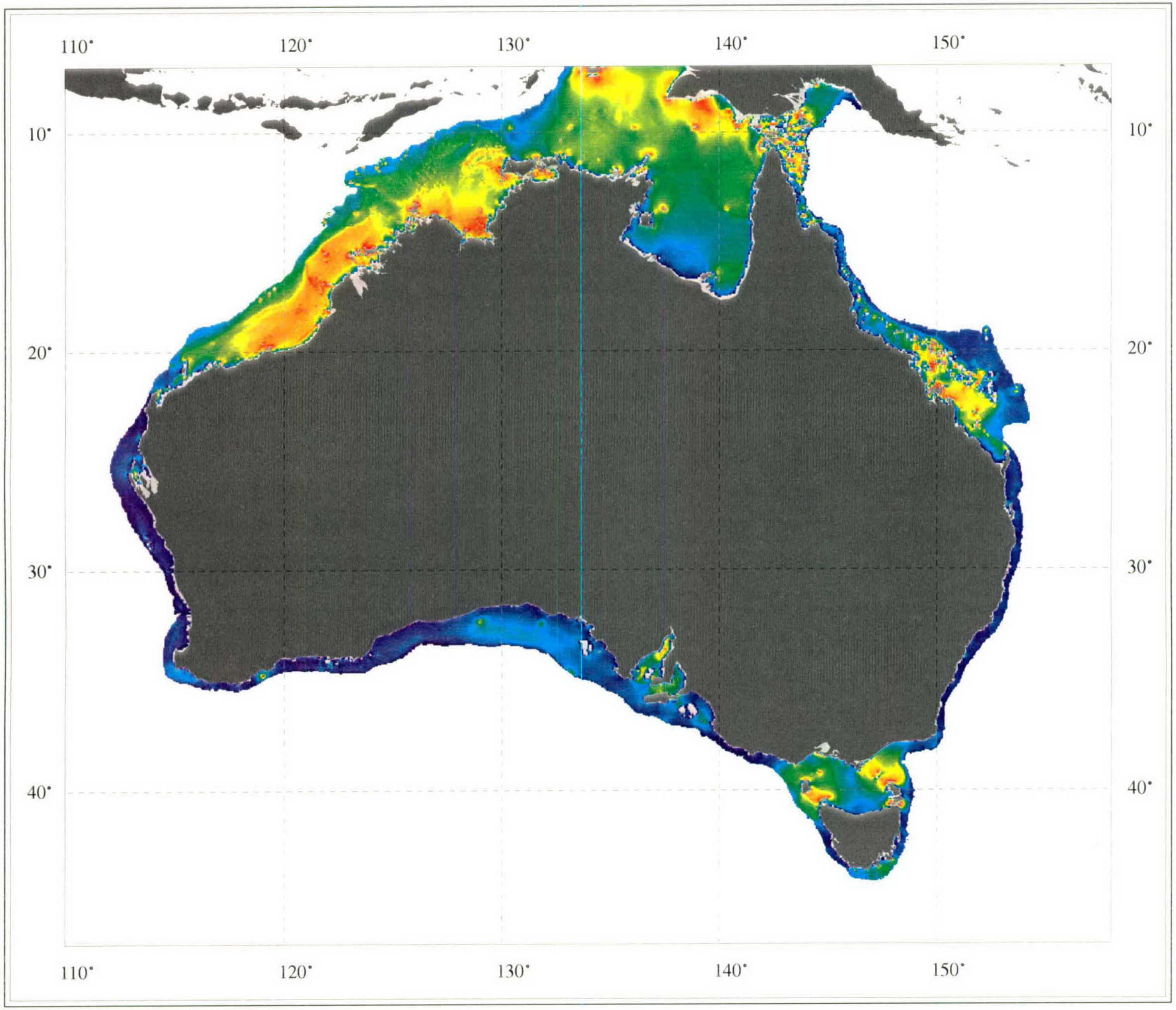

Figure 11.

Maximum Tidal Current

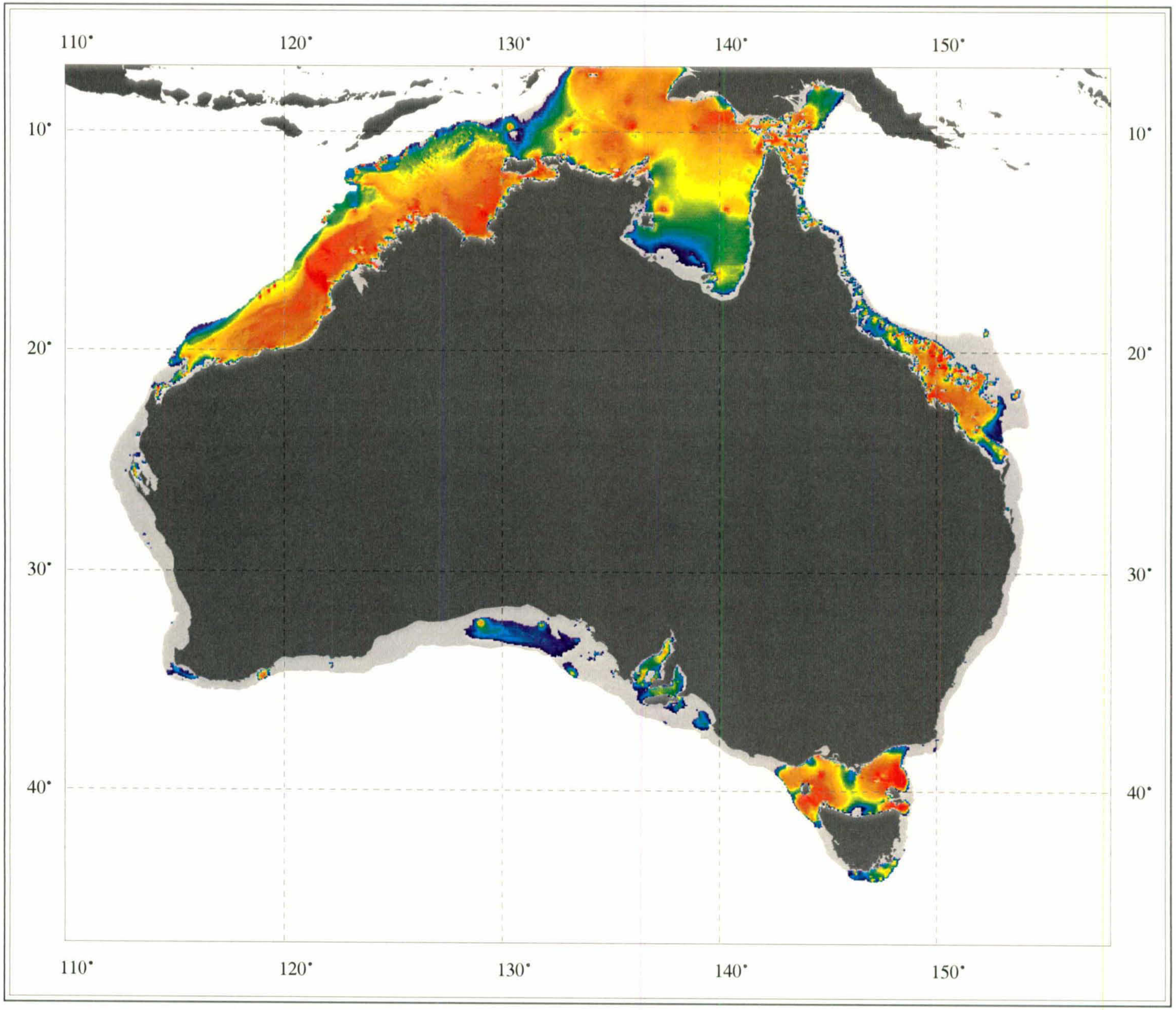

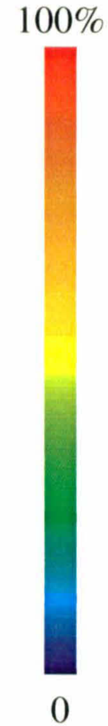

Figure 12A.

Tidal Induced Exceedance 0.01 mm grain size.

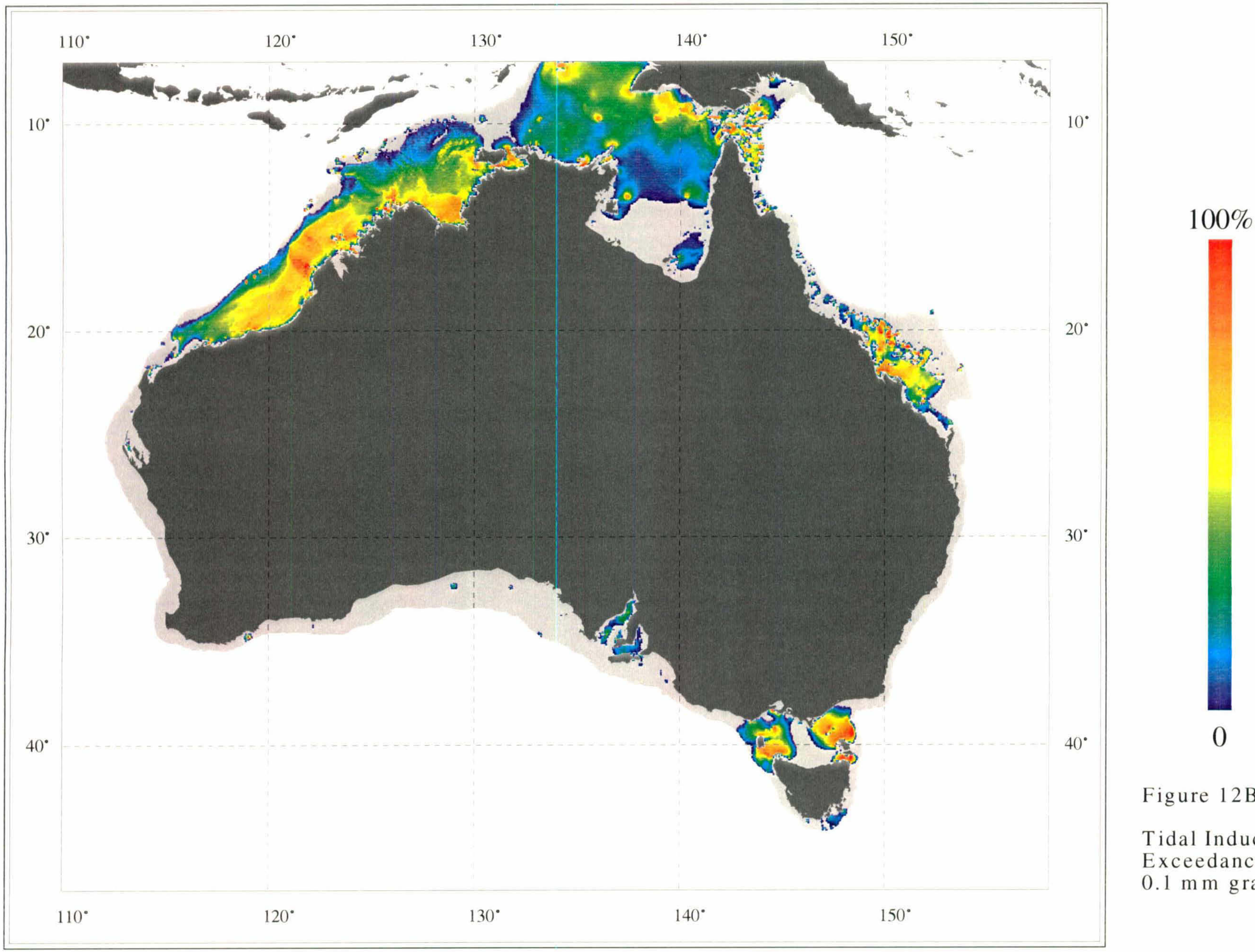

Figure 12B.

Tidal Induced
Exceedance
0.1 mm grain size.

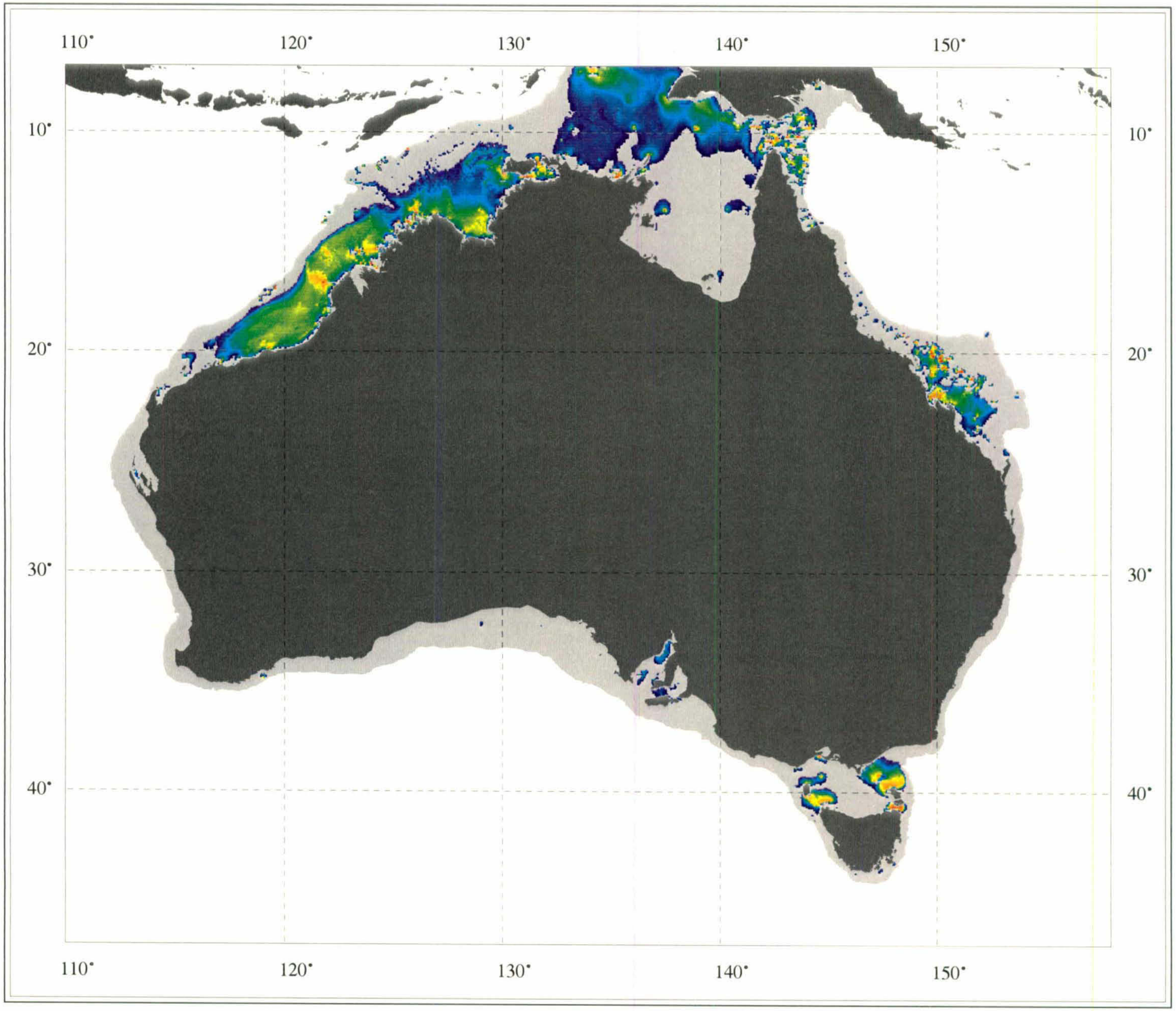

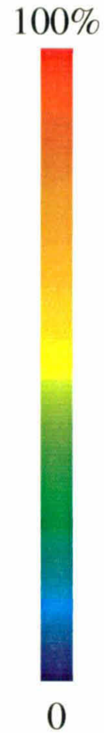

Figure 12C.

Tidal Induced Exceedance 0.5 mm grain size.

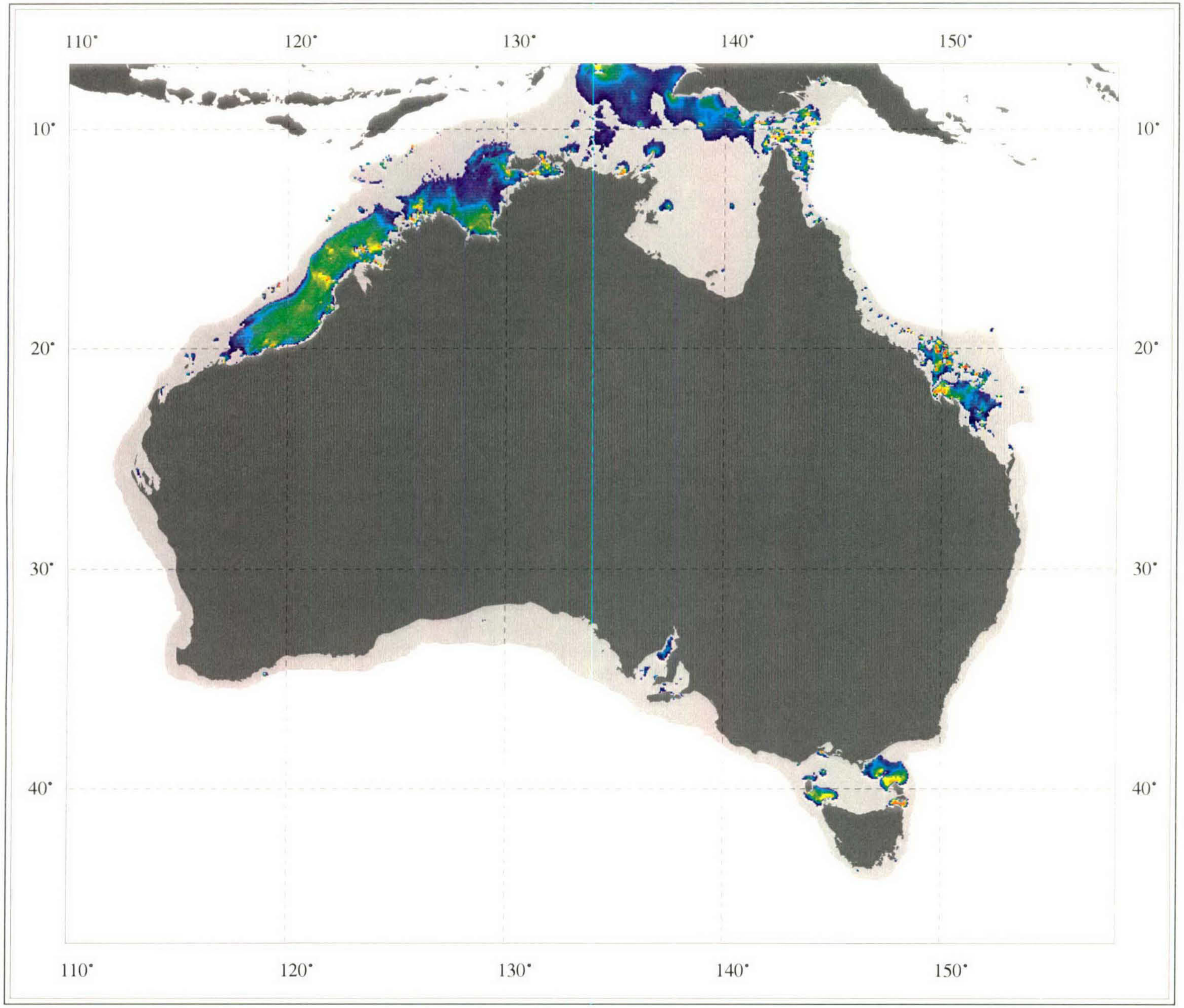

Figure 12D.

Tidal Induced
Exceedance
1.0 mm grain size.

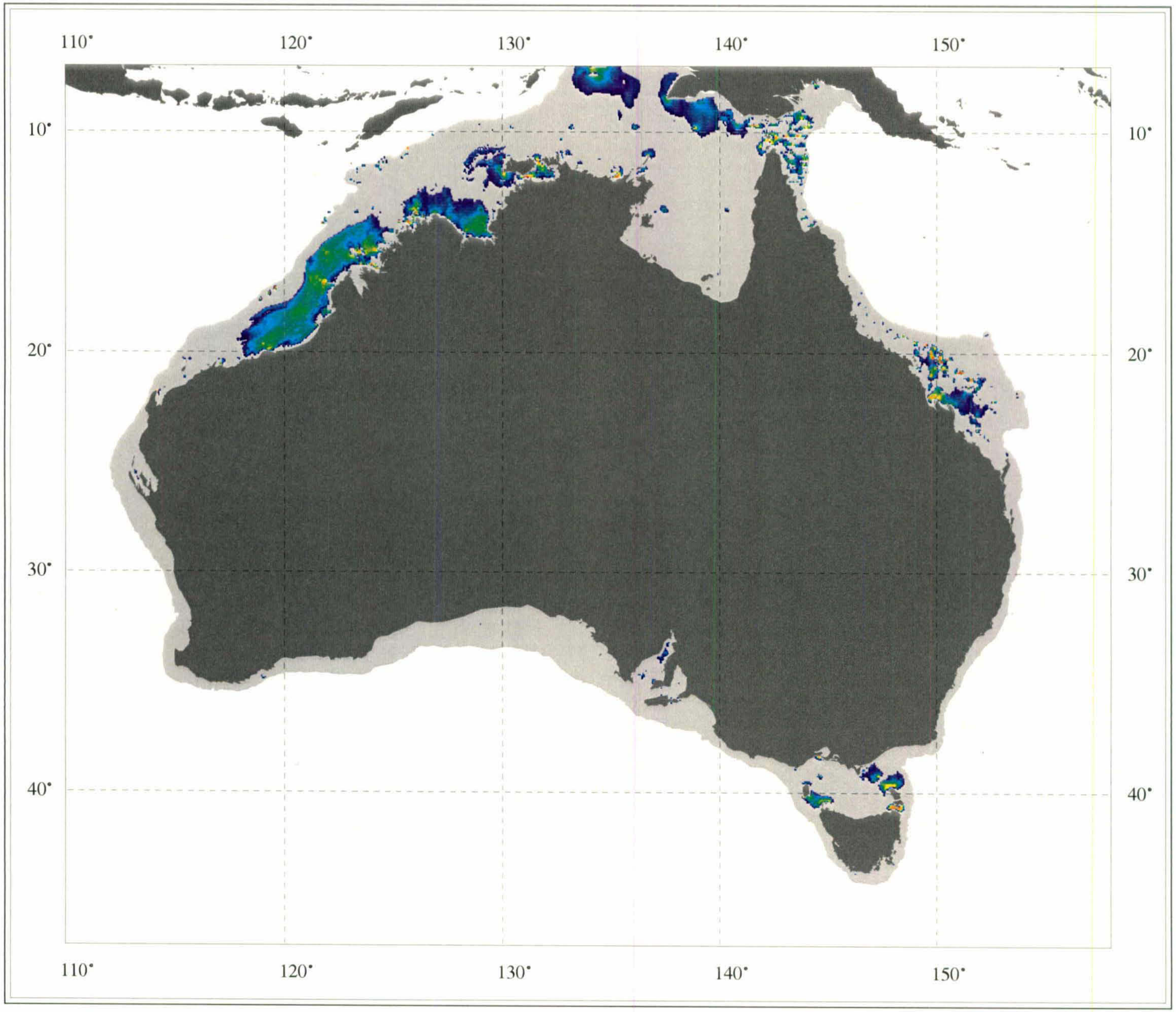

Figure 12E.

Tidal Induced Exceedance 2.0 mm grain size.

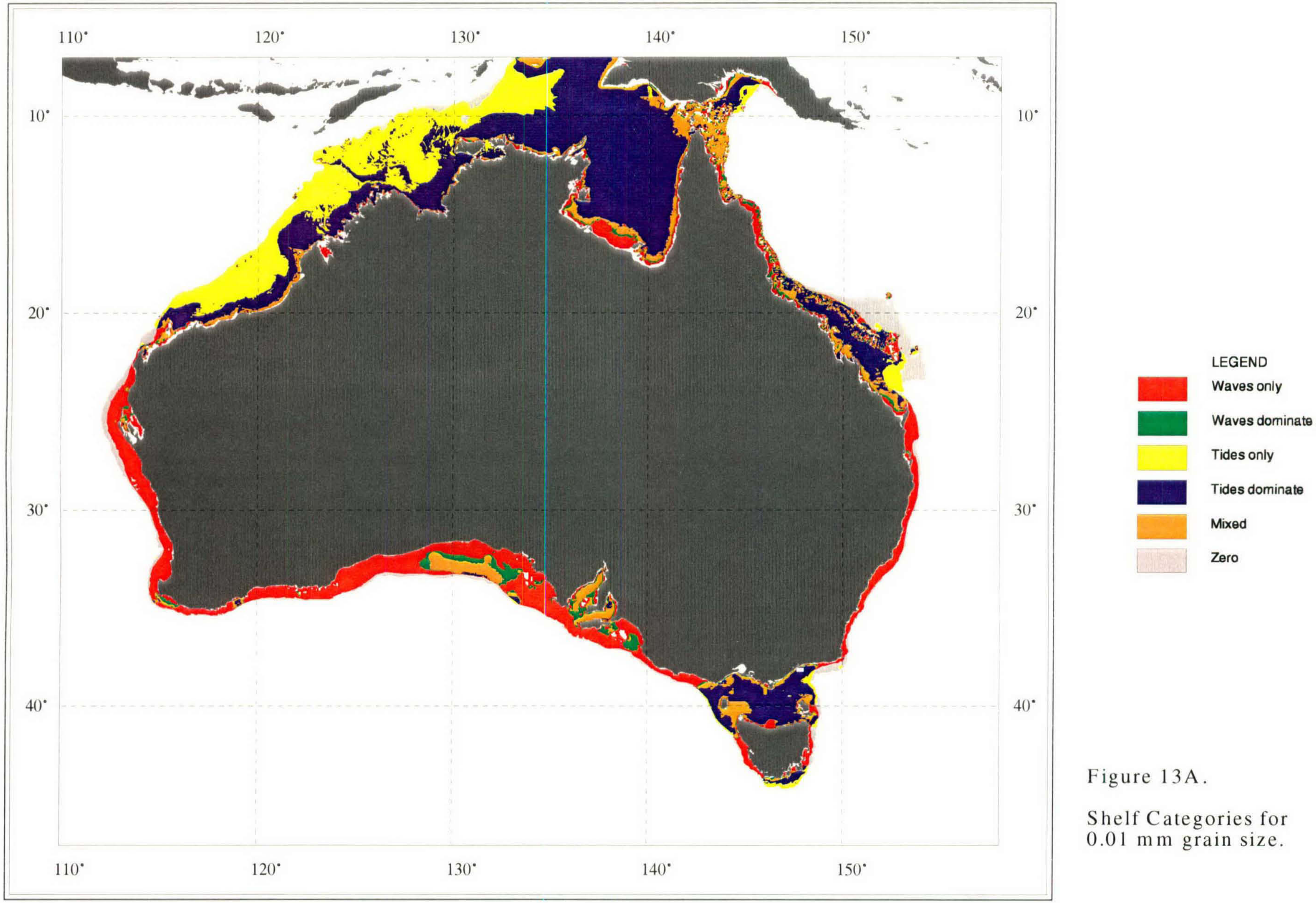

Figure 13A.

Shelf Categories for 0.01 mm grain size.

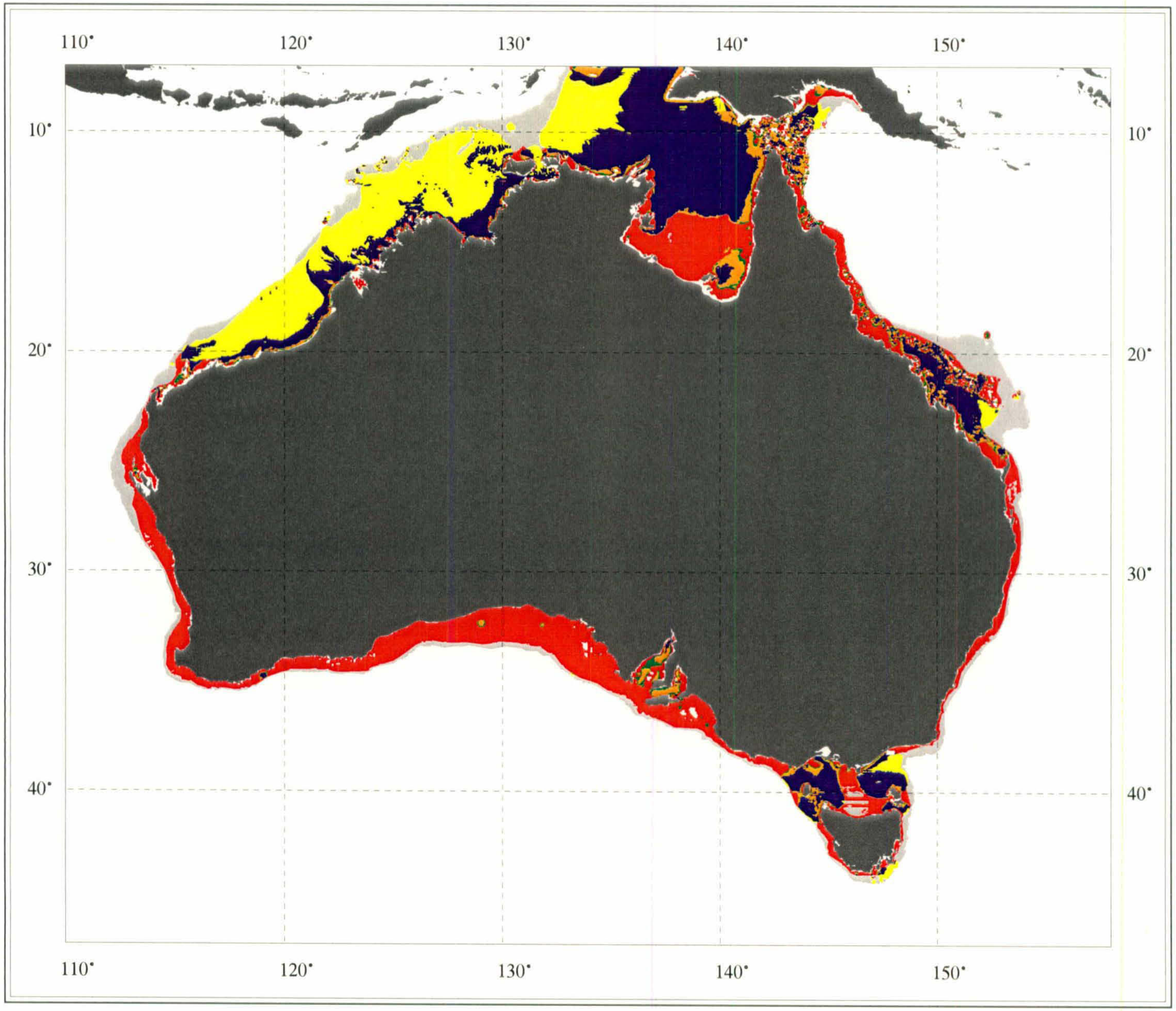

Figure 13B.

Shelf Categories for 0.1 mm grain size.

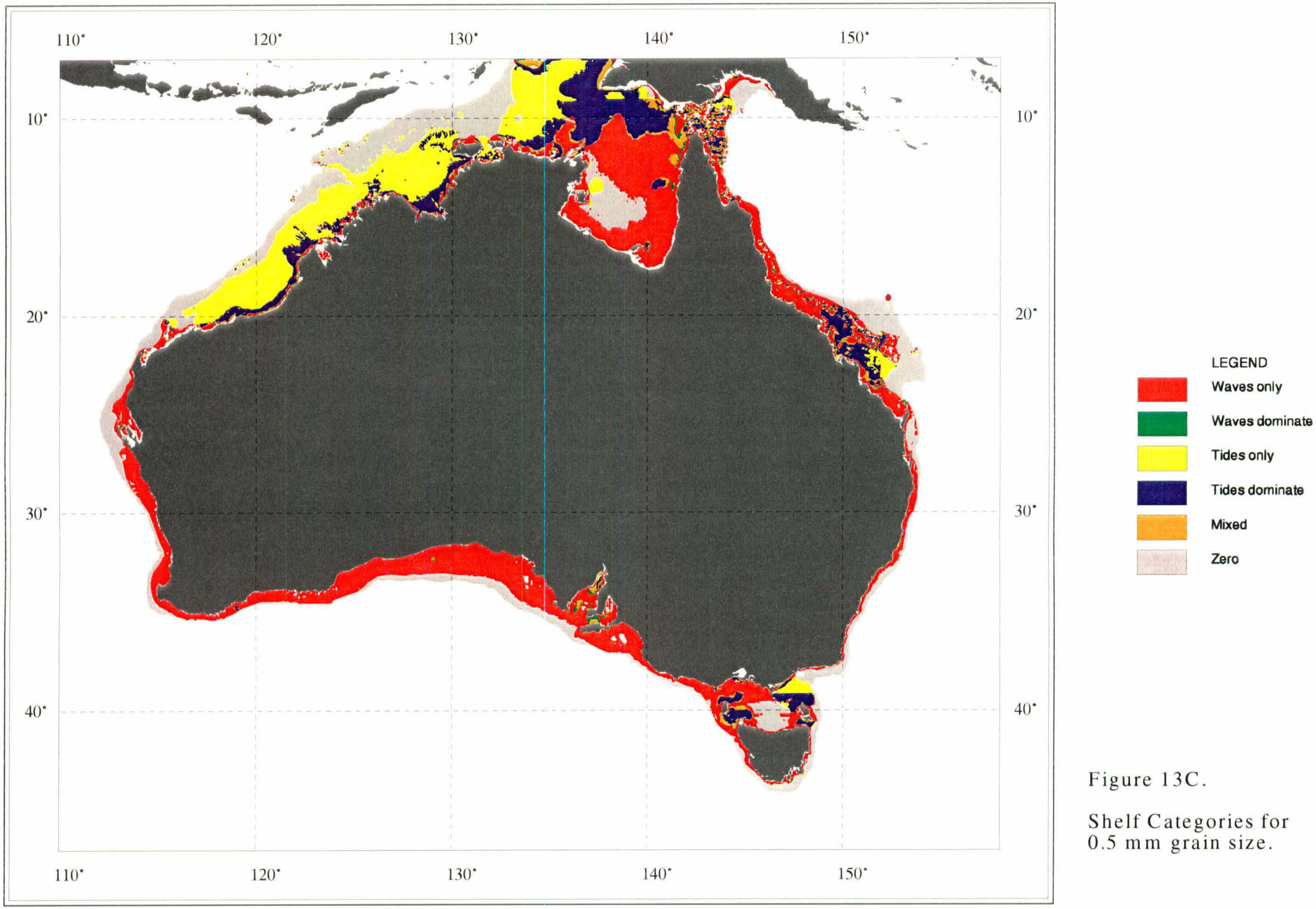

Figure 13C.

Shelf Categories for 0.5 mm grain size.

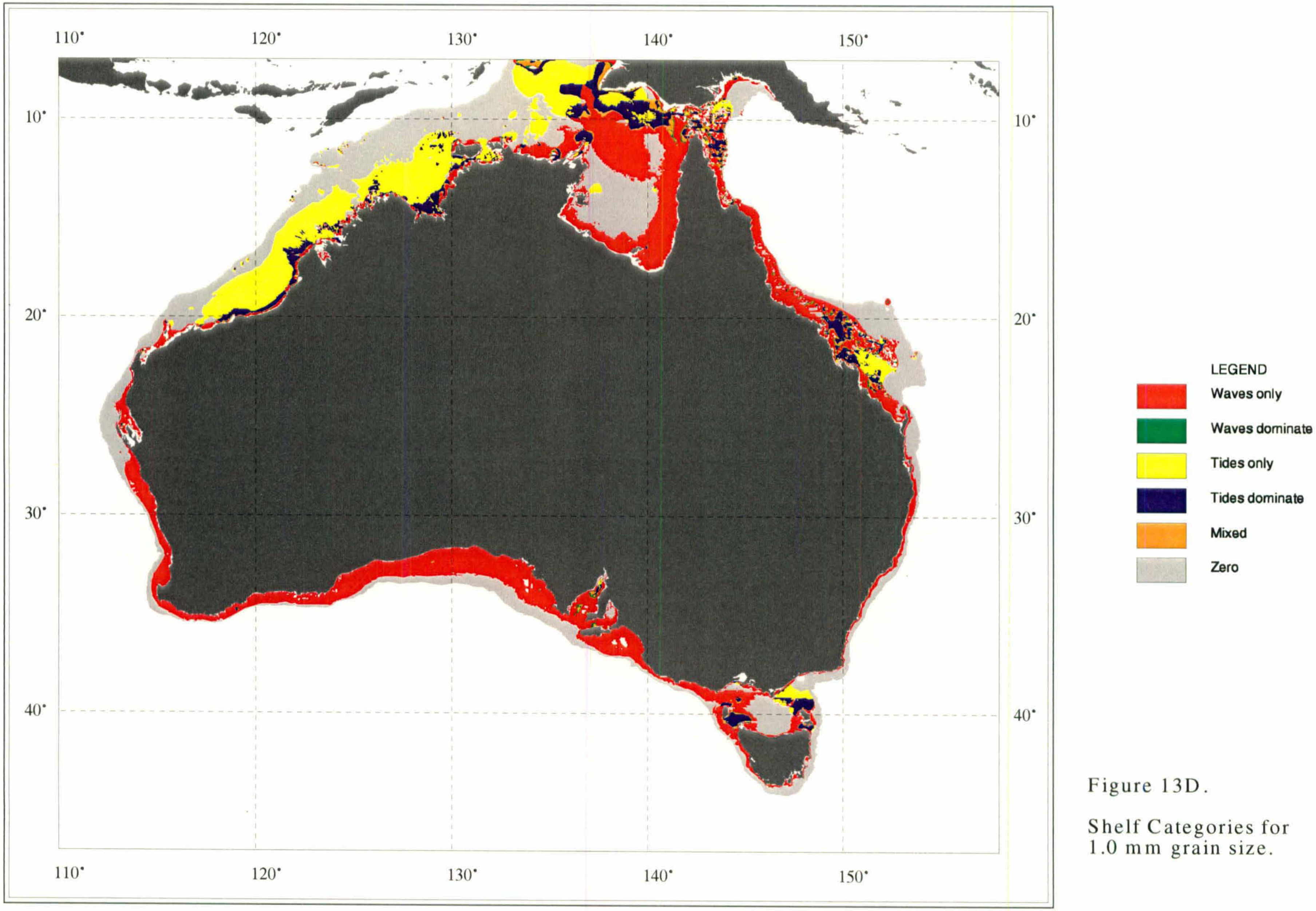

Figure 13D.

Shelf Categories for 1.0 mm grain size.

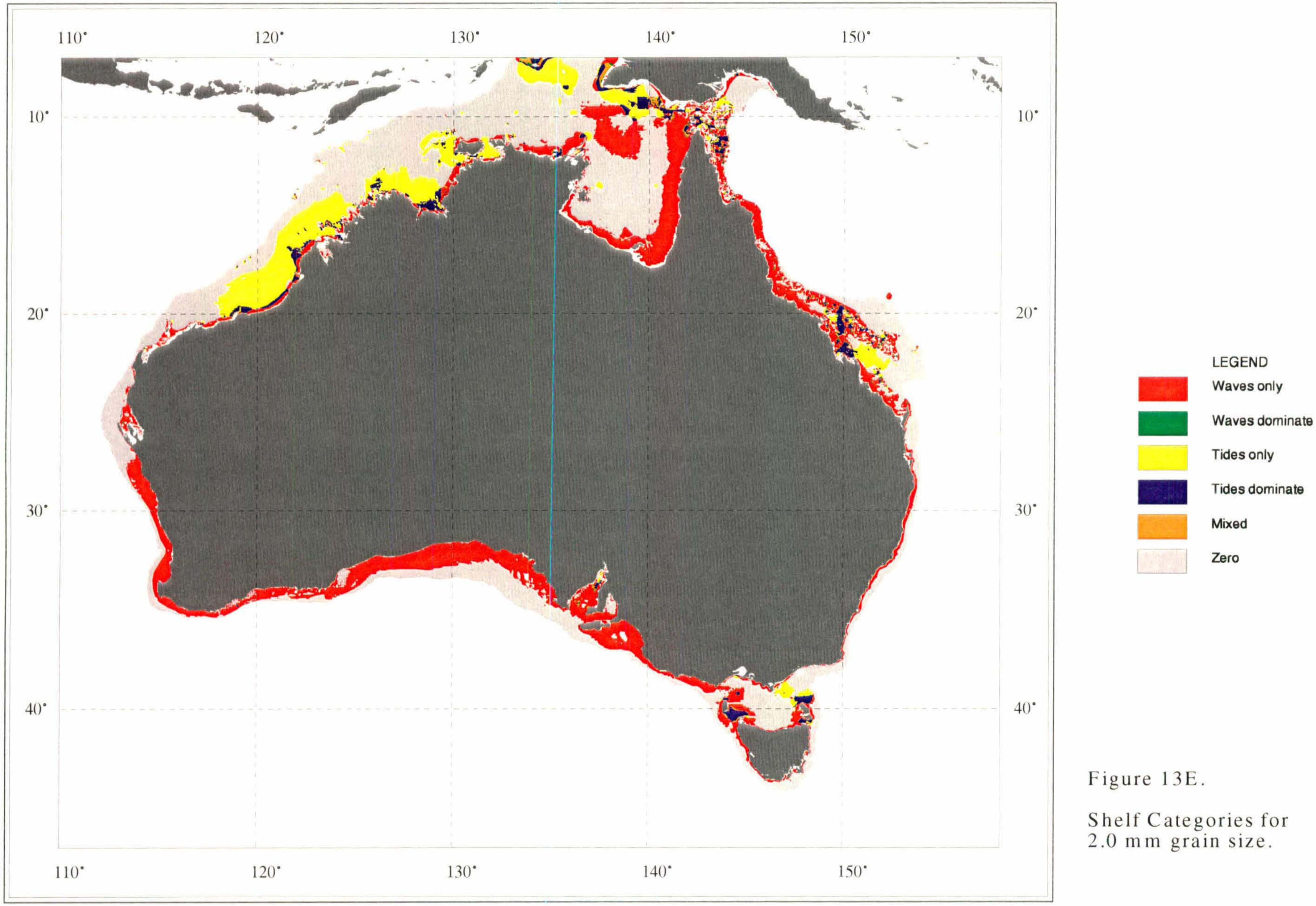

Figure 13E.

Shelf Categories for 2.0 mm grain size.

Tidal currents are also relatively strong in some mesotidal (2-4 m mean spring tidal range) and microtidal (< 2m) gulfs and shelf seaways, such as the Gulf of Carpentaria, Spencer Gulf, Gulf of St. Vincent, Bass Strait and Torres Strait. Amphidromic points located in the Gulf of Carpentaria, Joseph Bonaparte Gulf and in Bass Strait (Harris 1994) are locations of tidal current maxima (Fig. 11). Smaller embayments and estuaries may also exhibit tidal dominance locally (eg. Moreton Bay, Port Phillip Bay, Shark Bay, King Sound, etc.) but such smaller systems are not considered in this report.

The modelling results indicate that strong tidal currents occur on the shelf adjacent to southern Irian Jaya. Very few field studies have been carried out in this region (Wolanski, 1993), so it is difficult to verify this result.

3.2.2 *Threshold exceedence due to tides*

The modelling results indicate that fine sand (0.1 mm) is mobilised by tidal currents at least once during a neap-spring cycle over 56.4% of the Australian continental shelf. For gravel (2mm) the result is around 17.5% (Table 2). The spatial distribution of tidal threshold exceedence (Fig. 12) illustrates that tidal currents are competent to entrain finer sediments in the silt to fine sand range over most of the northern and northeastern sections of the shelf, in Bass Strait, Shark Bay and in Spencer Gulf. Gravel, on the other hand, is only mobilised locally (Fig. 12E), mainly on the inner shelf at the sites of strongest tidal flows mentioned above.

3.3 Shelf classification based on the wave/tidal exceedence ratio

In the final part of our analysis, we have attempted to combine the wave and tidal exceedence estimates into a ratio that gives some insight into the relative importance of these two processes in mobilising shelf bottom sediments. Overlaying the results shown in Figures 9 and 12, we have defined 6 separate categories of continental shelf types (Figs. 13A to E). The first category includes all areas of the shelf where neither wave nor tidal currents were competent in mobilising the bottom sediments (ie a "zero" or no-movement category). The second two categories are areas where only one process was competent in mobilising the bottom sediments (ie waves only or tides only).

Table 2. Shelf areas where threshold is exceeded by tidal currents for five grain size classes.

% Exceedence	Area (km^2)	%Shelf	Grain Size (mm)
<=1%	20800	0.82	0.01
>1, <=10%	140800	5.53	0.01
>10, <=50%	570500	22.42	001
> 50, <100%	1143300	44.92	0.01
100%	4300	0.17	001
<=1%	32700	1.28	0.1
>1, <=10%	248800	9.78	0.1
>10, <=50%	846500	33.26	0.1
> 50, <100%	308300	12.11	0.1
100%	200	0.01	0.1
<=1%	38000	1.49	0.5
>1, <=10%	340700	13.39	0.5
>10, <=50%	505100	19.85	0.5
> 50, <100%	45200	1.78	0.5
100%	0	0.00	0.5
<=1%	52200	2.05	1.0
>1, <=10%	286800	11.27	1.0
>10, <=50%	327800	12.88	1.0
> 50, <100%	19600	0.77	1.0
100%	0	0.00	1.0
<=1%	45100	1.77	2.0
>1, <=10%	189600	7.45	2.0
>10, <=50%	200200	7.87	2.0
> 50, <100%	9800	0.39	2.0
100%	0	0.00	2.0

The final three categories are all characterised by a mixture of wave and tidal threshold exceedence. In these areas, both processes are competent to mobilise the grain size in question. Whereas it is a simple matter to report where tides are competent in mobilising the bottom sediments more often than waves, it is not as obvious that such locations would be dominated by tides and tidal processes. The problem arises where the ratio of wave/tide percentage time of exceedence is close to to unity. For example, at locations where waves and tides are both competent in mobilising bottom sediments for 30% of the time, the energy regime is neither tide or wave dominated. Rather, such an area would constitute a "mixed" energy regime. This concept of mixed wave and tidal current energy in mobilising bottom sediments is well established in the literature (eg. Grant and Madsen, 1979, 1986; Pattiaratchi and Collins, 1985; Lyne et al., 1990). The question is, what is the meaning of the term "dominance" in relation to tidal and wave processes, given the available data and its spatial/temporal limitations.

For the purposes of the present study, we have defined as "dominant" a process that is at least three times more effective than another, thus distinguishing between tide-dominated, wave-dominated and mixed regimes. Our definition of *wave-dominated* applies to locations where the percentage of time of wave mobilisation is greater than 3 times the percentage of time of tide mobilisation; *tide-dominated* applies to locations where the percentage of time of tidal mobilisation is greater than 3 times the percentage of time of wave mobilisation; and mixed locations are where the ratio of wave/tidal percent time exceedence is between 1/3 and 3.

Examination of the spatial distribution of these categories (Fig. 13) illustrates that the category boundaries change depending upon the reference grain size. For example, the area of western Bass Strait between Tasmania and King Island is shown as a mixed regime for silt and fine sand (Fig. 13A and B), but as a tidally dominated area for coarse sand and gravel. The areas of shelf where the "zero" (no-motion) category applies increases with increasing grain size (Table 3), from 7% of the shelf for silt (0.01 mm) to 57% of the shelf for gravel (2mm).

Perhaps a less obvious result is that the relative percentage of the shelf that is tides-only and tide-dominated is around 60% (three times the amount for waves-only and wave-dominated) for silt, but for coarse sand and gravel the situation reversed (the wave area is twice that of the tides; see Table 3). This is explained from the tidal neap-spring cycle. Whereas silt and fine sand may be mobilised for a significant part of the time, gravel and coarse sand will only be mobilised during spring tides (and then only whilst the tidal flow is close to its maximum). On neap tides and slack water (minimum tidal current speed) tides are generally not competent to mobilise sand or gravel. Since we have registered exceedence as a percentage of time, the ratio of wave/tide exceedence is skewed in favour of waves for the coarser grain sizes.

Overall, there is a fairly good correspondence between the present results (Fig. 13) and the regionalisation attempted by Harris (1995; Fig. 3). For example, Figure 3 shows that about 17% of the Australian shelf is dominated by tidal currents, which corresponds closely to the estimate for gravel in the present study, which is 16.5% (sum of tide-only and tide-dominated). The correspondence between the spatial distribution of the two regionalisations is also fairly good (cf. Figs. 3 and 13) although there are some disparities. Bass Strait, for example, is shown in Figure 3 as dominated by swell waves, whereas our results shows areas of tidal dominance for all grain sizes (Fig. 13 A-E).

Table 3. Shelf areas of six different energy regime categories in relation to five grain size classes.

Category	Area km^2	%Shelf	Grain Size (mm)
wave only	482700	18.97	0.01
wave dom	70800	2.78	0.01
tide dom	1066200	41.89	0.01
tide only	503500	19.78	0.01
mixed	239200	9.40	0.01
zero	182700	7.18	0.01
wave only	732000	28.76	0.1
wave dom	34400	1.35	0.1
tide dom	721900	28.36	0.1
tide only	552500	21.71	0.1
mixed	127700	5.02	0.1
zero	376600	14.80	0.1
wave only	895300	35.18	0.5
wave dom	14900	0.59	0.5
tide dom	351800	13.82	0.5
tide only	489100	19.22	0.5
mixed	73200	2.88	0.5
zero	720800	28.32	0.5
wave only	827100	32.50	1.0
wave dom	7100	0.28	1.0
tide dom	190600	7.49	1.0
tide only	450500	17.70	1.0
mixed	38200	1.50	1.0
zero	1031600	40.53	1.0
wave only	646400	25.40	2.0
wave dom	3500	0.14	2.0
tide dom	91700	3.60	2.0
tide only	330100	12.97	2.0
mixed	19400	0.76	2.0
zero	1454000	57.13	2.0

4. DISCUSSION

There are a number of factors affecting the nature and distribution of sediments on the continental shelf, including (past and present) shelf energy regime, climate, sea level change, sediment supply, morphology, biology and chemistry (Fig. 14). These factors are inter-related in terms of their effect on shelf sediments. Although in this report we have focussed on the shelf energy regime, it is emphasised that the true value of this knowledge is not only to better understand the processes and patterns of shelf sediment mobilisation themselves, but to better understand the functioning of the shelf environment as a system (NASA, 1988).

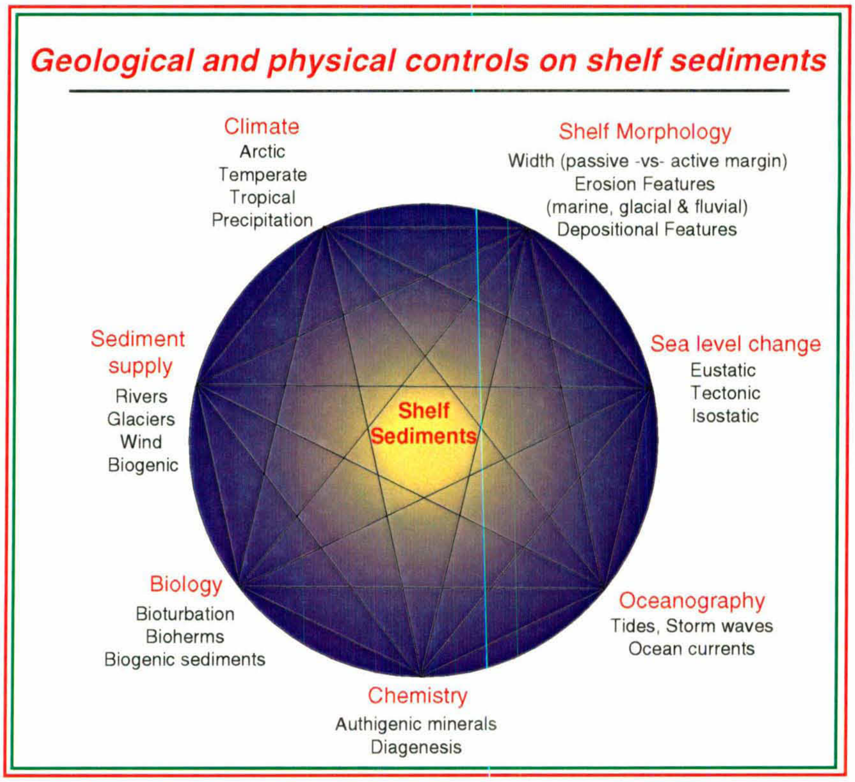

Figure 14. Diagram showing the major geological and physical factors influencing the nature of shelf sediments. Lines join factors of interrelated influence.

4.1 GEOMAT as a Management Tool

Partially because of the interconnectedness of the shelf sediment system (Fig. 14), we consider that GEOMAT has applications to a number of areas beyond physical sedimentology. Foremost among these include the use of shelf regionalisations for management purposes because of the relationship between sediment mobility zones and habitats. Sedimentologists generally focus on the preserved fossil assemblage and rarely consider the entire suite of living organisms that may be associated with a given core site or sedimentary environment. Biologists are equally biased in their research work, as much more has been published on hard substrate ecosystems (rocky shores and coral reefs) than on soft sediments (Gray, 1981). Nonetheless, a few specific studies have been carried out that link sediment types to ecosystems. For example, Somers (1987) has shown that there is a relationship between percentage of terrigenous mud in bottom sediments and the distribution of commercial prawn species in the western Gulf of Carpentaria. Long et al (1995) described the megabenthos in the Gulf of Carpentaria as comprising two communities, one associated with coarse sandy sediments and another with muddier deposits. In Torres Strait, different seagrass and faunal communities are developed in relation to tidally-induced bottom stress maxima (B. Long, pers comm) such as are shown in Figure 3. Shepherd (1983) described the structure of epifaunal communities which inhabit migrating dunes in Spencer Gulf. Recently, Roy et al. (in prep.) have proposed that different assemblages of species (flora and fauna) are associated with the specific estuarine environments.

The regionalisations shown in Figure 13 thus have implications for the distribution of specific benthic habitats. In combination with other information on sediment properties, seafloor roughness and biological communities, these regionalisations may provide the basis for extrapolating from smaller to wider areas. For example, the high energy, mixed and tide-dominated zones of eastern and western Bass Strait are also known to comprise coarse-grained carbonate dunes (also termed "sandwaves") which spatially coincide with a large part of the preferred trawl-grounds for commercial scallop fishermen in Bass Strait (Kailola et al., 1993). In other words, the habitat type in this area is in part linked to the physical processes controlling sediment mobilisation.

4.2 Significance of "zero" (no-motion) zones

Although the present study has focussed on near-bed currents generated by tidal

and swell-wave processes, shelf currents occur at a number of different spatial and temporal scales: at the scale of turbulence (0.2-5 sec); at the scale of wave orbital currents (5-20 sec); at the scale of tidal currents (6 hours); and at the scale of storm events (6-10 days). Superimposed upon these "events" will be other currents, such as intruding ocean currents (Fig. 3) which may flow at a steady rate for weeks or months without changing significantly in speed or direction. The current regime in any given area is the product of a combination of different current components, although one type may be dominant locally (eg. Swift et al., 1971; see Fig. 15). However, there are areas of the shelf where the total energy available to mobilise the bottom sediment is very low (ie where even the processes shown in Figure 15 acting in combination are weak).

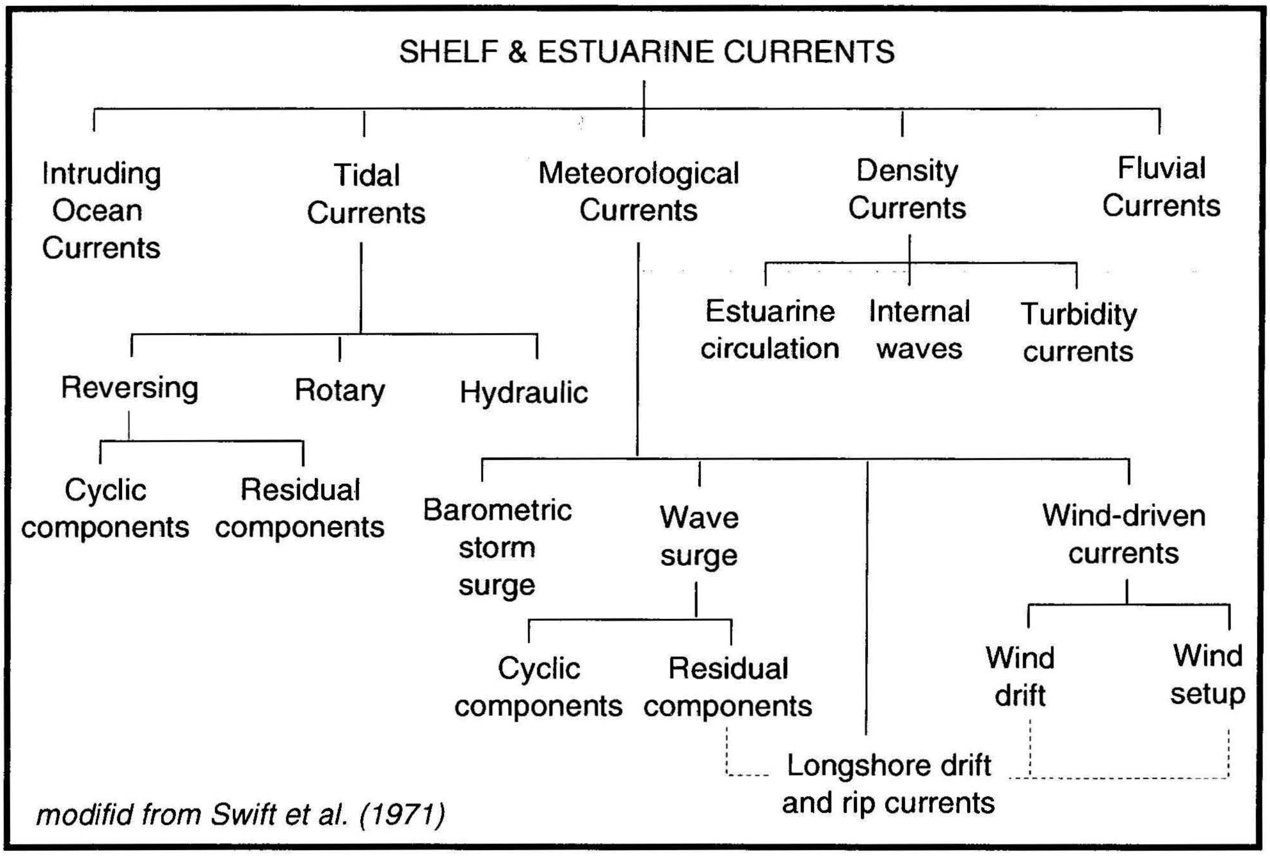

Figure 15 Diagram showing types of currents that influence sediment mobility on the continental shelf.

Depending on the grain size selected, our results indicate that significant areas of the shelf experience wave and tidal regimes that are not competent in initiating sand transport (Fig. 13). Although such areas may be influenced by oceanographic processes other than waves and tides (eg. Fig. 15), to a first approximation they may be considered to be low-energy, depositional environments. Sediments deposited in such low-energy areas are probably bioturbated and relatively high in mud content, as explained by Aigner's (1985) "proximality" diagram. These quiescent depositional areas are of special interest to environmental managers because inputs of contaminants to such areas are likely to cause more severe impacts in comparison with other, more energetic, shelf environments. Quiet depocentres are limited in their capacity to disperse (and dilute) anthropogenic contaminants. For example, fine-grained muddy sediments are more likely to be correlated with heavy metals (eg. Bourg, 1987). Hence, the highest levels of heavy metals are found to accumulate in the muddy deposits of Spencer Gulf (Harbison, 1984) the Torres Strait (Baker et al., 1991), and Sydney Harbour (Birch and Irvine, 1998).

4.3 Future Work

GEOMAT has applications to any seafloor engineering projects, where knowledge of seafloor stability is necessary. Examples include cable laying, pipeline construction, shipping channel dredging and maintenance, and other applications where the mobilisation of the seabed sediments is a relevant factor (eg. RAN requirements for mine clearance operations). A recent project to lay a power-cable across Bass Strait (BASSLINK) benefited from analyses carried out using GEOMAT, which was able to differentiate sections of the route where sand mobilisation was likely to cause scouring problems (where more expensive burial of the cable might be necessary; Harris et al., 1999). We envisage that future applications of GEOMAT will be to solve problems for such engineering applications as well as meeting the needs of environmental managers and studies of anthropogenic material dispersal in the shelf sedimentary system.

We consider that using wave and tide models to predict sediment threshold exceedence usefully identifies shelf areas where sediments may be mobilised. However, we freely admit our approach has ignored several factors complicating where mobilisation actually occurs. Some factors will diminish the estimated areas of exceedence. Actual shelf sediments are rarely cohesionless quartz spheroids; rather, they are commonly a cohesive, angular, poorly sorted mixture of gravel, sand and mud and have a complex origin (Shepard, 1963; Swift and Thorne, 1991) and they are often transported across continental shelves and to locations where they are in equilibrium with the hydrodynamic regime (Nitterouer and Wright, 1994). Thus, by using a uniform assumed grain size, areas of mobilisation are most probably overestimated. The wave and tidal threshold equations used here ignores the frictional drag of bed roughness elements such as bedforms, rocky pinnacles, etc.; where such roughness elements occur we will have overestimated threshold exceedence. The WAM wave model we used is considered to perform well in the open sea, and the high resolution grid used here (11 km) will represent features of about that scale. However, it cannot account for bathymetrically complex features such as small (<11 km) reefs, islands or sand bars. Wave sheltering, diffraction and refraction around such small obstacles may reduce the wave energy, and hence our data might be expected to overestimate exceedence in the vicinity of such features.

Other factors will increase the areas of mobilisation. The shelf hydrodynamic regime comprises ocean currents, internal waves, wind-driven flows and other currents superimposed upon tidal currents and surface swell waves (Fig. 15). In nature, swell waves and tidal currents do not act in isolation, but rather they combine together and with other currents to mobilise sand (Grant and Madsen, 1979, 1986; Pattiaratchi and Collins, 1985; Lyne et al., 1990) and hence our estimates are conservative, because any additional currents would increase the areas of threshold exceedence.

The benefit is that simplified models as used here permit a continent-wide approach that provides a more general insight into natural shelf sedimentary processes. By treating the tides and waves separately in the present study, we were able to examine the relative importance of each process individually, which would not be possible when combined waves and tides are analysed. In future analyses we plan to combine swell wave and tidal currents to estimate sand transport intensity over the continental shelf using mean grain size estimations provided by Sydney University's AUSEABED database.

Eventually, we will add model output to include the effects of ocean currents on sediment threshold exceedence. Examples of shelf sand transport under ocean currents have been documented form the South African shelf (Flemming 1978), the Brazil shelf (Adams et al. 1986), the Japan shelf (Ikehara and Yasumasa 1994)) and the East Antarctic shelf (Harris and O'Brien, 1998). On the Australian continental shelf Harris et al. (1996) described the mobilisation of rhodolith gravel in up to 80 m water depth offshore of Fraser Island under the influence of the East Australia Current. Harris (1995) speculates that the Leeuwin Current may affect the mobilisation of sand off North West Cape, WA. The significance of ocean currents as agents of shelf sand transport is difficult to assess from the available information. It seems likely that using computer models of ocean currents would make a useful contribution towards addressing this problem.

5. CONCLUSIONS

The GEOMAT computer modelling project has generated regionalisations of the Australian continental shelf, differentiating between swell wave and tidally dominated shelf environments. The modelling predicts that swell wave energy is sufficient to mobilise fine sand (0.01 mm diameter), on at least one occasion during the year March 1997 to February 1998, over 63.5% of the Australian continental shelf. The largest and most powerful waves were able to mobilise fine sand up to a water depth of 148 m in the Great Australian Bight. Tidal currents are capable of mobilising fine sand at least once per semi-lunar cycle (ie. ~2 weeks) over about 56.4% of the shelf.

Overlaying the wave and tide threshold exceedence maps demonstrates that there are areas on the shelf where one of the process dominates, some areas where the processes are of relatively equal importance and still other areas where neither process is significant. In order to assess the spatial distribution of these different areas, we defined 6 shelf regions of relative wave and tidal energy: zero (no-mobility); waves-only, wave-dominated, mixed, tide-dominated and tides-only. To classify as a wave dominated area, the percentage of time of wave exceedence had to be more than 3 times the percentage of time of tidal current exceedence. Areas which failed to meet this criteria fell into the "mixed" category. The relative distribution of these regions varies with the selection of different grain sizes, but the overall pattern is not too dissimilar from the conceptually-based regionalisation proposed by Harris (1995). Improvements to the model that are being considered include better resolution of tidal currents in the coastal zone (<20 m water depth) and inclusion of estimated mean grain size into the models.

The regionalisations derived using GEOMAT provide a predictive, process-based understanding of the shelf sedimentary system. It explains the distribution patterns of surficial sediments and will probably be useful for mapping biological habitats and communities, although further work is needed to better define these relationships. GEOMAT provides a useful tool that will assist with marine environmental management in general, and with the National Ocean's Office regional marine planning process in particular. It has demonstrated applications to marine engineering projects where shelf sediment mobilisation is of concern and to regional studies of pollution dispersal and accumulation in quiescent, low-energy shelf depocentres.

ACKNOWLEDGEMENTS

This work was financially supported by the Cooperative Research Centre for the Antarctic and Southern Ocean Environment, University of Tasmania and by the Australian Geological Survey Organisation. Thanks to Drs J. Blevin, V. Passlow and J. Colwell for providing critical reviews of an earlier version of this report. Published with the permission of the Chief Executive Officer, Australian Geological Survey Organisation.

REFERENCES

Adams, C. E., Wells, J. T., and Coleman, G. T. (1986). Transverse bedforms on the Amazon shelf. *Continental Shelf Research*, 6, 175-187.

Aigner, T., (1985). *Storm depositional systems*. Lecture Notes in Earth Sciences No. 3, Berlin, Springer-Verlag, 174 p.

Anderson, O. B., Woodworth, P. L. and Flather, R. A. (1995). Intercomparison of recent global ocean tide models. *Journal of Geophysical Research*. 100(C12), 25261-25282.

Baker, E. K., and Harris, P. T. (1991). Copper, lead and zinc in the sediments of the Fly River Delta and Torres Strait. *Marine Pollution Bulletin.*, 22(12), 614-618.

Black, K. P., and Oldman, J. W. (1999). Wave mechanisms responsible for grain sorting and non-uniform ripple distribution across two moderate-energy, sandy continental shelves. *Marine Geology*, 162, 121-132.

Boreen, T., James, N. P., Wilson, C., and Heggie, D. (1993). Surficial cool-water carbonate sediments on the Otway continental margin, southeastern Australia. *Marine Geology*, 112, 35-56.

Bourg, A.C.M., (1987). Trace metal adsorption modelling and particle water interactions in estuarine environments. Continental Shelf Research, 7: 1319-1332.

Birch, G. F., and Irvine, I. (1998). Distribution of heavy metals in surficial sediments of Port Jackson, Sydney, New South Wales. *Australian Journal of Earth Science*, 45(2), 297-304.

Church, J. A., and Forbes, A. M. G. (1983). Circulation in the Gulf of Carpentaria, I, direct observations of currents in the southeast corner of the Gulf of Carpentaria. *Aust. J. Mar. Freshwater Res.*, 34, 1-10.

Clifton, H.E., and Dingler, J.R., (1984). Wave formed structures and paleoenvironmental reconstruction. *Marine Geology*, 60: 165-198.

Collins, L. B. (1988). Sediments and history of the Rottnest Shelf, southwest Australia: a swell-dominated, non-tropical carbonate margin. *Sediment. Geol.*, 60, 15-49.

Cook, P. J., and Mayo, W. (1978). *Sedimentology and Holocene history of a tropical estuary (Broad Sound, Queensland)*. Australian Bureau of Mineral Resources Bulletin, 170, 206 pp.

Davies, A.G., (1985). Field observations of the threshold of sediment motion by wave action. *Sedimentology*, 32: 685-704.

Davies, P. J. (1979). *Marine geology of the continental shelf off southeast Australia*. Bureau of Mineral Resources Bulletin 195, 51 pp.

de Pablo, C. L., de Agar, P. M., Barturen, R., Nicolas, J. P., and Pineda, F. D. (1994). Design of an information system for environmental planning and management (SIPA). *Journal of Environmental Management*, 40, 231-243.

Easton, A. K. (1970). *The tides of the continent of Australia.* Adelaide, Horace Lamb Centre for Oceanographic Research, 326 pp.

Flemming, B. W. (1978). Underwater sand dunes along the southeast African continental margin - observations and implications. *Marine Geology*, 26, 177-198.

Gagan, M. K., Chivas, A. R., and Herczeg, A. L. (1990). Shelf wide erosion, deposition and suspended sediment transport during cyclone Winifred, central Great Barrier Reef, Australia. *Journal of Sedimentary Petrology*, 60(3), 456-470.

Garratt, J.R. (1992). *The Atmospheric Boundary Layer*, Cambridge Univ. Press, Cambridge, U.K., 316pp.

Gordon, A. D., and Hoffman, J. G. (1986). Sediment features and processes of the Sydney continental shelf. In E. Frankel, J. B. Keene, and A. E. Waltho (Eds.), *Recent Sediments in Eastern Australia, Marine Through Terrestrial* Sydney, Geological Society of Australia, NSW Division, pp. 29-52.

Grant, W. D., and Madsen, O. S., (1979). Combined wave and current interaction with a rough bottom. *Journal of Geophysical Research*, 84 (C4): 1797-1808.

Grant, W. D., and Madsen, O. S., (1986). The continental-shelf bottom boundary layer. *Annual Review of Fluid Mechanics*, 18: 265-305.

Green, M. O., Vincent, C. E., McCave, I. N., Dickson, R. R., Rees, J. M., and Pearson, N. D., (1995). Storm sediment transport: observations from the British North Sea shelf. *Continental Shelf Research*, 15(8): 889-912.

Gray, J. S. (1981). *The ecology of marine sediments.* Cambridge Studies in Modern Biology, Cambridge, Cambridge University Press, 185 pp.

Hammond, T. M., and Collins, M. B., (1979). On the threshold of sand-sized sediment under the combined influence of unidirectional and oscillatory flow. *Sedimentology*, 26: 795-812.

Harbison, P. (1984). Regional variation in the distribution of trace metals in modern intertidal sediments of northern Spencer Gulf, South Australia. *Marine Geology.*, 61, 221-247.

Hardisty, J., (1994). Beach and nearshore sediment transport. In K. Pye (Editor), *Sediment transport and depositional processes*. Blackwell, Oxford, pp. 219-255.

Harris, P.T., (1994). Comparison of tropical, carbonate and temperate, siliciclastic tidally dominated sedimentary deposits: examples from the Australian continental shelf. *Australian Journal of Earth Science*, 41: 241-254.

Harris, P. T. (1995). Marine geology and sedimentology of the Australian continental shelf. In L. P. Zann and P. Kailola (Eds.), *The State of the Marine Environment Report for Australia Technical Annex 1: The Marine Environment* Canberra, Department of the Environment, Sport and Territories, pp. 11-23.

Harris, P. T., and Coleman, R. (1998). Estimating global shelf sediment mobility due to swell waves. *Marine Geology*, 150, 171-177.

Harris, P. T., and O'Brien, P. E. (1998). Bottom currents, sedimentation and ice-sheet retreat facies successions on the Mac.Robertson shelf, East Antarctica. *Marine Geology*, 151, 47-72.

Harris, P. T., Pattiaratchi, C. B., Collins, M. B., and Dalrymple, R. W. (1995). What is a bedload parting? In B. W. Flemming and A. Bartholoma (Eds.), *Tidal signatures in modern and ancient sediments* Oxford, Blackwell, IAS Special Publication No. 24, pp. 1-18.

Harris, P. T., Tsuji, Y., Marshall, J. F., Davies, P. J., Honda, N., and Matsuda, H. (1996). Sand and rhodolith-gravel entrainment on the mid- to outer-shelf under a western boundary current: Fraser Island continental shelf, eastern Australia. *Marine Geology*, 129, 313-330.

Harris, P. T., Smith, R., and O'Brien, P. E. (1999). *Report on BASSLINK cable route in Bass Strait: Seabed geology, bathymetry, and sediment mobilisation.* Report prepared for: William Wood and Associates Pty Ltd, Environmental Management Consultants, Relbia, TAS. Australian Geological Survey Organisation, 43 pp.

Hasselman, K., and WAMDI Group, (1988). The WAM model - A third generation ocean wave prediction model. Journal of Physical Oceanography, 18: 1775-1810.

Hearn, C. J., and Holloway, P. E. (1990). A three-dimensional barotropic model of the response of the Australian North West Shelf to tropical cyclones. *Journal of Physical Oceanography.*, 20, 60-80.

Ikehara, K., and Yasumasa, K. (1994). Distribution and origin of subaqueous dunes on the shelf of Japan. *Marine Geology*, 120, 75-87.

James, N. P., Bone, Y., Von Der Borch, C., and Gostin, V. A. (1992). Modern carbonate and terrigenous clastic sediments on a cool water, high energy, mid-latitude shelf: Lacepede, southern Australia. *Sedimentology,* 39, 877-903.

Johnson, M. A., Kenyon, N. H., Belderson, R. H., and Stride, A. H. (1982). Chapter 4. Sand Transport. In A. H. Stride (Eds.), *Offshore Tidal Sands* London, Chapman and Hall, pp. 58-94.

Jones, H. A., and Kudras, H. R. (1982). SONNE SO-15 cruise 1980 off the east coast of Australia - bathymetry and seafloor morphology. *Geol. Jb.*, D56, 55-67.

Kachel, N. B., and Smith, J. D., (1989). Sediment transport and deposition on the Washington continental shelf. In: M. R. Landry and B. M. Hickey (Eds.), *Coastal Oceanography of Washington and Oregon*. Amsterdam, Elsevier, pp. 287-348.

Kailola, P. J., Williams, M. J., Stewart, P. C., Reichelt, R. E., McNee, A., & Grieve, C. (1993). *Australian Fisheries Resources*, Bureau of Rural Resources, Canberra. 422 pp.

Kershaw, P. J., Swift, D. J. P., Pentreath, R. J., and Lovett, M. B., (1984). The incorporation of plutonium, americium, and curium into the Irish Sea sea bed by biological activity. *Science of the Total Environment*, 40: 61-81.

Komar, P.D., and Miller, M.C., (1973). The threshold of sediment movement under oscillatory water waves. *Journal of Sedimentary Petrology*, 43: 1101-1110.

Komen, G., Cavaleri, L., Donelan, M., Hasselman, K., Hasselman, S., and Janssen, P.A.E.M., (1994). *Dynamics and Modelling of Ocean Waves*: Cambridge, Cambridge University Press, 532 p.

Long, B. G., Poiner, I. R., and Wassenberg, T. J. (1995). Distribution, biomass and community structure of megabenthos of the Gulf of Carpentaria, Australia. *Marine Ecology Progress Series*, 129, 127-139.

Louis, J. P., and Radok, J. R. M. (1975). Propagation of tidal waves in the Joseph Bonaparte Gulf. *Journal of Geophysical Research,* 80(12), 1689-1690.

Lyne, V.D., Butman, B., and Grant, W.D., 1990. Sediment movement along the U.S. east coast continental shelf - I. Estimates of bottom stress using the Grant-Madsen model and near-bottom wave and current measurements. *Continental Shelf Research*, 10: 397-428.

McMillan, J. D. (1982). *A Global Atlas of GEOS-3 Significant Waveheight Data and Comparison of the Data with National Buoy Data* No. 156882). NASA, Wallops Flight Center, Virginia.

Madsen, O.S., (1994). Spectral wave-current bottom boundary layer flows. *Proceedings of the 24th International Conference on Coastal Engineering*, Coastal Engineering Research Council/ASCE, Kobe, Japan, pp. 384-398.

Malikides, M., Harris, P. T., Jenkins, C. J., and Keene, J. B. (1988). Carbonate sandwaves in Bass Strait. *Australian Journal of Earth Science*, 35, 303-311.

Miller, M. C., McCave, I. N., and Komar, P. D. (1977). Threshold of sediment motion under unidirectional currents. *Sedimentology,* 24, 507-527.

NASA (1988). *Earth System Science: a closer view.* Washington DC, National Aeronautics and Space Administration, 208 pp.

Nittrouer, C. A., and Wright, L. D., (1994). Transport of particles across continental shelves. *Reviews of Geophysics*, 32(1): 85-113.

Pattiaratchi, C.B., and Collins, M.B., (1985). Sand transport under the combined influence of waves and tidal currents: an assessment of available formulae. *Marine Geology*, 67: 83-100.

Pingree, R. D., and Griffiths, D. K. (1979). Sand transport paths around the British Isles resulting from M2 and M4 tidal interactions. *Journal of the Marine Biological Association U. K.*, 59, 497-513.

Puri, K., Dietachmayer, G.S., Mills, G.A., Davidson, N.E., Bowen, R.A. and Logan, L.W. (1998). The new BMRC Limited Area Prediction System, LAPS, *Australian Meteorological Magazine,* 47: 203 - 233.

Rennie, H., Bierwirth, P., and Scott, G. (1997). Torres Strait satellite image of the sea floor. 1:300,000 scale, Australian Geological Survey Organisation. Canberra ACT.

Roy, P. S., Williams, R. J., Jones, A. J., Coates, B., Gibbs, P. J., Yassini, I., Hudson, J. P., and West, R. J. (submitted). Structure and function of southeast Australian estuaries. *Australian Journal of Earth Sciences.*

Seaman, R., Bourke, W., Steinle, P., Hart, T., Embery, G., Naughton, M. and Rikus L. (1995). Evolution of the Bureau of Meteorology's Global Assimilation and Prediction System, Part 1: Analyses annd Initialization, *Australian Meteorological Magazine.*, 44, 1 - 18.

Shepard, F.P. (1963). *Submarine Geology.* New York, Harper and Row, 557 p.

Shepherd, S.A. (1983). The epifauna of megaripples: species' adaptions and population responses to disturbance. *Australian Journal of Ecology*, 8, 3-8.

Sherwood, C. R., Butman, B., Cacchione, D. A., Drake, D. E., Gross, T. F., Sternberg, R. W., Wiberg, P. L., and Williams III, A. J., (1994). Sediment transport events on the northern California continental shelf during the 1990-1991 STRESS experiment. *Continental Shelf Research*, 14: 1063-1099.

Somers, I. F. (1987). Sediment type as a factor in the distribution of commercial prawn species in the western Gulf of Carpentaria, Australia. *Australian Journal of Marine and Freshwater Research,* 38, 133-149.

Sternberg, R. W. (1972). Predicting initial motion and bedload transport of sediment particles in the shallow marine environment. In D. J. P. Swift, D. B. Duane, and O. H. Pilkey (Eds.), *Shelf Sediment Transport* Stroudsburg, PA, Dowden, Hutchinson and Ross Inc., pp. 61-82.

Swift, D. J. P., Stanley, D. J., and Curray, J. R. (1971). Relict sediments, a reconsideration. *Journal of Geology*, 79, 322-346.

Swift, D. J. P., Han, G., and Vincent, C. E. 1986. Fluid processes and sea-floor response on a modern storm-dominated shelf: middle Atlantic shelf of North America. Part 1: The storm-current regime. In R. J. Knight and J. R. McLean (Eds.), *Shelf Sands and Sandstones*, Canadian Society of Petroleum Geologists, Calgary, pp. 99-119.

Swift, D.J.P., and Thorne, J.A., (1991). Sedimentation on continental margins, I: a general model for shelf sedimentation. *Special Publication of the International Association of Sedimentologists*, 14: 3-31.

Vincent, C. E., (1986). Processes affecting sand transport on a storm-dominated shelf. In: R. J. Knight and J. R. McLean (Editors), *Shelf Sands and Sandstones* Calgary, Candian Society of Petroleum Geologists, pp. 121-132.

Walker, R.G., (1984). Shelf and shallow marine sands. In: Walker, R.G., ed., *Facies Models*: Toronto, Geological Association of Canada, p. 141-170.

Walker, R.G., and James, N.P. (Ed.). (1992). *Facies Models: response to sea level change*. St Johns, Newfoundland: Geological Association of Canada, pp. 409.

Wolanski, E. (1985). Some properties of waves at the Queensland shelf break. In *7th Australasian Conference on Coastal and Ocean Engineering*, 2 (pp. 61-70). Christchurch, N.Z.:

Wolanski, E. (1993). Water circulation in the Gulf of Carpentaria. *Journal of Marine Systems*, 4, 401-420.

Wolanski, E., and Eagle, A. M. (1991). Oceanography and sediment transport, Fly River Estuary and Gulf of Papua. In *10th Australasian Conference on Coastal and Ocean Engineering*, . Aukland, New Zealand: pp. 453-457.

Appendix

Reprint of: Harris, P. T and Coleman, R. (1998). Estimating global shelf sediment mobility due to swell waves. *Marine Geology*, 150: 171-177.